



**NMRF/VR/03/2023**



सत्यमेव जयते

**VERIFICATION REPORT**

**NCUM Global Model Verification:  
Pre-monsoon (MAM) 2023**

**K. Niranjana Kumar, Sukhwinder Kaur, M. Venkatarami Reddy, Harvir Singh, Sushant Kumar, Anumeha Dube, Mohana S. Thota, and Raghavendra Ashrit**

**2023**

**National Centre for Medium Range Weather Forecasting  
Ministry of Earth Sciences, Government of India  
A-50, Sector-62, NOIDA-201 309, INDIA**

**NCUM Global Model Verification:  
Pre-monsoon (MAM) 2023**

**K. Niranjan Kumar, Sukhwinder Kaur, M. Venkatarami Reddy, Harvir Singh, Sushant Kumar, Anumeha Dube, Mohana S. Thota, and Raghavendra Ashrit**

**NMRF/VR/03/2023**

**National Centre for Medium Range Weather Forecasting  
Ministry of Earth Sciences, Government of India  
A-50, Sector 62, NOIDA-201309, INDIA  
[www.ncmrwf.gov.in](http://www.ncmrwf.gov.in)**

## Data Control Sheet

1	Name of the Institute	National Center for Medium range Weather Forecasting
2	Document Number	NMRF/VR/03/2023
3	Date of Publication	November 2023
4	Title of the document	NCUM Global Model Verification: Pre-monsoon (MAM) 2023
5	Type of the document	Verification Report
6	Number of pages, figures, and Tables	45 pages, 32 figures, 4 Tables
7	Authors	K. Niranjana Kumar, Sukhwinder Kaur, M. Venkatarami Reddy, Harvir Singh, Sushant Kumar, Anumeha Dube, Mohana S. Thota, and Raghavendra Ashrit
8	Originating Unit	National Centre for Medium Range Weather Forecasting (NCMRWF), A-50, Sector-62, NOIDA201 309, India.
9	Abstract	This report provides a comprehensive assessment of the NCMRWF's NCUM global model analysis and forecast performance during the Pre-monsoon season (MAM) of 2023. Aimed at both forecasters and model developers, the verification results are presented with a focus on biases in forecasted winds, temperature, humidity, and rainfall. These crucial insights enable forecasters to effectively interpret the model guidance, aiding in accurate and informed weather forecasting. The findings also offer valuable feedback to model developers, supporting continuous improvement efforts to enhance the model's forecasting capabilities.
10	References	17
11	Security classification	Unrestricted
12	Distribution	General

## Table of Contents

S.No		P.No.
	<b>Abstract</b>	1
<b>1.</b>	<b>Introduction</b>	2
<b>2.</b>	<b>NCMRWF Unified Modelling System &amp; Verification datasets</b>	2
	<i>2.1. Model Description</i>	2
	<i>2.2. Observed/analysis Data used for the verification</i>	3
<b>3.</b>	<b>NCUM-G Analysis Mean and Anomalies during MAM 2023</b>	4
	<i>3.1. Winds at 850, 700, 500, and 200 hPa levels</i>	4
	<i>3.2. Temperature at 850, 700, 500, and 200 hPa levels</i>	6
	<i>3.3. Relative Humidity (RH) at 850, 700, and 500 hPa levels</i>	8
<b>4.</b>	<b>Systematic Errors in NCUM-G Forecasts</b>	10
	<i>4.1. Winds at 850, 700, 500, and 200 hPa levels</i>	10
	<i>4.2. Temperature and Relative Humidity</i>	14
	<i>4.3. Surface (10m) winds</i>	20
	<i>4.4. Temperature at 2m</i>	21
	<i>4.5. Total Precipitable Water (PWAT)</i>	22
<b>5.</b>	<b>Forecast Verification during MAM 2023</b>	23
	<i>5.1. Rainfall Mean and Mean Error</i>	24
	<i>5.2. Categorical Scores of Rainfall Forecasts</i>	24
	<i>5.3. Categorical Scores of Tmax</i>	24
<b>6.</b>	<b>Significant Weather during MAM 2023</b>	27
	<i>6.1. Bay of Bengal ESCS 'MOCHA' during 9-15 May 2023</i>	27
	<i>6.1.1. Forecast Tracks and Strike Probability</i>	28
	<i>6.1.2. Forecast Track Errors</i>	29
	<i>6.1.3. Forecast Intensity Errors (Min SLP and Max Wind)</i>	31
	<i>6.1.4. Forecast Landfall Error</i>	32
	<i>6.1.5. Verification of Strike Probability</i>	33
	<i>6.1.6. CRA Verification of Rainfall forecasts</i>	33
	<i>6.2. Western Disturbance &amp; Heat Waves</i>	36
	<i>6.2.1. Western Disturbances</i>	36
	<i>6.2.2. Heat Waves</i>	38
	<i>6.2.3. Observed and forecasted daily Tmax time series</i>	40
<b>7.</b>	<b>Summary</b>	41
<b>8.</b>	<b>References</b>	45

# NCUM Global Model Verification: Pre-monsoon (MAM) 2023

**K. Niranjan Kumar, Sukhwinder Kaur, M. Venkatarami Reddy, Harvir Singh, Sushant Kumar, Anumeha Dube, Mohana S. Thota, and Raghavendra Ashrit**

## सारांश

यह रिपोर्ट 2023 के प्री-मॉनसून सीज़न (मार्च से मई) के दौरान रा.म.अ.मौ.पू.के. के एन.सी.यू.एम वैश्विक मॉडल विश्लेषण और पूर्वानुमान प्रदर्शन का व्यापक मूल्यांकन प्रदान करती है। पूर्वानुमानकर्ताओं और मॉडल डेवलपर्स दोनों के उद्देश्य से, सत्यापन परिणाम पूर्वानुमानित तापमान, आर्द्रता, वर्षा, और हवाओं में पूर्वाग्रहों पर ध्यान केंद्रित करके प्रस्तुत किए जाते हैं। ये महत्वपूर्ण अंतर्दृष्टि पूर्वानुमानकर्ताओं को मॉडल मार्गदर्शन की प्रभावी ढंग से व्याख्या करने में सक्षम बनाती हैं, जिससे सटीक और सूचित मौसम पूर्वानुमान में सहायता मिलती है। निष्कर्ष मॉडल डेवलपर्स को मूल्यवान प्रतिक्रिया भी प्रदान करते हैं, जो मॉडल की पूर्वानुमान क्षमताओं को बढ़ाने के लिए निरंतर सुधार प्रयासों का समर्थन करते हैं।

## Abstract

This report provides a comprehensive assessment of the NCMRWF's NCUM global model analysis and forecast performance during the Pre-monsoon season (MAM) of 2023. Aimed at both forecasters and model developers, the verification results are presented with a focus on biases in forecasted winds, temperature, humidity, and rainfall. These crucial insights enable forecasters to effectively interpret the model guidance, aiding in accurate and informed weather forecasting. The findings also offer valuable feedback to model developers, supporting continuous improvement efforts to enhance the model's forecasting capabilities.

## **1. Introduction**

This comprehensive report documents the performance evaluation of the global NCMRWF Unified Model (NCUM-G) forecasts during the Pre-monsoon season (MAM) of 2023. The primary objective of this assessment is to verify the accuracy and reliability of the forecasts by comparing them against model analyses and observations. Through meticulous verification, the results are skillfully summarized, shedding light on the average biases, and forecast performances for the entire season. Given the diverse audience, the report is thoughtfully oriented towards both forecasters and model developers, recognizing their distinct interests in understanding and improving the forecasting process. Sections 3 to 5 of the report delve into the systematic biases found in the forecasted large-scale upper fields, encompassing crucial elements such as wind, temperature, humidity, and rainfall, among others. The insights provided in these sections prove to be invaluable in enabling forecasters to interpret the model forecasts more effectively and make informed decisions. Before delving into the forecast evaluation, Section 2 sets the foundation by presenting a comprehensive description of the NCUM-G model, including details about the sophisticated data assimilation system employed at NCMRWF. Moreover, this section offers insights into the observational datasets utilized in this study, ensuring transparency, and providing the context for the subsequent analyses. In Section 3, a detailed examination of the seasonal mean analysis and respective anomalies is presented, providing a holistic view of the model's performance throughout the Pre-monsoon season. Subsequently, Section 4 meticulously investigates the model's systematic errors, followed by a thorough validation of forecasts in section 5. One of the highlights of this report is covered in Section 6, where verification for significant weather events of MAM 2023 takes center stage. The verification process involves assessing the model's performance in predicting notable phenomena, including the Bay of Bengal extremely severe cyclonic system (ESCS) 'MOCHA' during 9-15 May 2023, Western Disturbances, and Heat Wave episodes. This analysis proves crucial for gauging the model's capabilities in capturing extreme weather events, which are often of immense significance to various stakeholders. Finally, Section 7 serves as a comprehensive culmination of the entire MAM 2023 report. It succinctly summarizes the key findings, strengths, and limitations of the NCMRWF model forecasts during this Pre-monsoon season. The summary offers valuable takeaways for both forecasters and model developers, aiding them in refining the forecasting process and enhancing the model's performance in subsequent seasons.

## **2. NCMRWF Unified Modelling System & Verification datasets**

### **2.1. Model Description**

NCMRWF started using the Unified Model (UM) Partnerships' seamless prediction system operationally since 2012 and this system was named NCUM. The NCUM global Numerical Weather Prediction (NWP) system (NCUM-G) become operational in 2012 with a grid resolution of 25 km (NCUM-G:V1) for medium-

range weather prediction. This was upgraded to 17 km horizontal resolution (NCUM-G:V3) in 2015, 12 km (NCUM-G:V5) in 2018, 12 km resolution with improved model physics in 2020 (NCUM-G:V6). The present version (NCUM-G: V7) of NCUM-G has a horizontal grid resolution of ~12 km with 70 vertical levels in the atmosphere reaching 80 km height. It uses “ENDGame” dynamical core, which provides improved accuracy of the solution of primitive model equations and reduced damping. This helps in producing finer details in the simulations of synoptic features such as cyclones, fronts, troughs, and jet stream winds. ENDGame also increases variability in the tropics, which leads to an improved representation of tropical cyclones and other tropical phenomena. The model uses improved physics options of GA7.2 (Walters et al., 2017). An advanced Data Assimilation (DA) method of Hybrid 4-Dimensional Variational (4D-Var) is used for the creation of NCUM global analysis. The advantage of the Hybrid 4D-Var is that it uses a blended background error, a blend of “climatological” background error, and day-to-day varying flow-dependent background error (derived from the 22–member ensemble forecasts). The hybrid approach is scientifically attractive because it elegantly combines the benefits of ensemble data assimilation (flow-dependent co-variances) with the known benefits of 4D-Var within a single data assimilation system (Barker, 2011). Various in-situ and remote-sensing observations are being used in the NCUM global DA system. New and novel observations are added to the DA system through in-house R&D and collaborations. A brief description of the NCUM Hybrid 4D-Var DA system is given in Kumar et al. (2021, 2020, & 2018). The surface analysis preparation system (SURF) prepares the surface analysis of snow, SST, sea ice, soil moisture, etc., for the NCUM-G model (SURF system includes Extended Kalman Filter based Land Data Assimilation System which is used for soil moisture analysis).

## **2.2. Observed/analysis Data used for the Verification**

The seasonal mean analysis and anomalies are studied using the fifth-generation European Centre for Medium-Range Weather Forecasts (ECMWF) reanalysis product (ERA-5) Hershbach et al., (2020) climatology (1979-2018). The high-resolution (12km) NCUM-G analysis data is interpolated to ERA-5 grid resolution ( $0.25^0 \times 0.25^0$ ). For verification of the forecasts, the NCUM-G model analysis is used. All systematic errors are computed at a native grid resolution of 12km.

Detailed quantitative rainfall forecast verification is based on the India Meteorological Department (IMD)-NCMRWF daily high-resolution ( $0.25^0$ ) rainfall analysis (Mitra et al. 2009, 2013). The rainfall analysis objectively analyses India Meteorological Department (IMD) daily rain gauge observations onto a  $0.25^0$  grid using a successive corrections technique with the GPM Satellite rainfall providing the first guess estimates. The model forecasts are gridded to the  $0.25^0$  observed rainfall grids over Indian land regions for 92 days from 1<sup>st</sup> March 2023 to 31<sup>st</sup> May 2023. As noted by Mitra et al. (2009), the merged analysis at  $0.25^0$  grid resolution

is appropriate for capturing the large-scale rain features associated with the monsoon. The merging of the IMD gauge data into GPM estimates not only corrects the mean biases in the satellite estimates but also improves the large-scale spatial patterns in the satellite field, which is affected by temporal sampling errors (Mitra et al. 2009). Verification of daily temperature forecasts is carried out against the IMD daily observed gridded ( $0.5^{\circ} \times 0.5^{\circ}$ ) maximum (Tmax) and minimum (Tmin) temperature data (Srivastava et al. 2009).

### **3. NCUM-G Analysis Mean and Anomalies during MAM 2023**

#### **3.1. Winds at 850, 700, 500, and 200 hPa levels**

The NCUM-G mean analysis fields and anomalies relative to climatology are assessed in this section during MAM 2023. The discussion is presented for Winds, Temperature, and Relative Humidity at four standard pressure levels of 850, 700, 500, and 200 hPa. The anomalies are computed against the fifth-generation European Centre for Medium-Range Weather Forecasts (ECMWF) reanalysis product (ERA5) climatology (1979-2018). The mean winds and anomalies at 850 and 700hPa levels from NCUM-G analysis are shown in Figures 1a-d. At 850 hPa and 700hPa, the NCUM-G model seasonal mean analysis represents northwesterly winds with increasing altitudes having magnitudes ranging from 5 to 10 m/s and the presence of anticyclone over the southern peninsular region. This anticyclonic circulation at 700 hPa level is clearly visible over the southern peninsular region in NCUM-G model analysis. The anomalous conditions for the MAM 2023 Pre-monsoon period are estimated by removing the climatological mean computed using ERA5 reanalysis from the NCUM-G seasonal mean winds. The anomalous winds at 850hPa and 700hPa are shown in Figures 1c-d. Wind anomalies indicate contrasting features in north and south with weaker and stronger winds in NCUM-G analysis with respect to ERA5 climatology, respectively, over the Indian subcontinent. At 850 hPa level, an anomalous cyclonic circulation is present over the Northwestern Indian regions. This circulation is becoming enhanced at 700 hPa level. On the other hand, over the equatorial Indian Ocean, specifically in southern latitudes, the winds are weaker in NCUM-G analysis resulting in strong anomalous easterlies. Overall, in the North India, the magnitude of winds is relatively lower compared to ERA5 climatology due to persistent anomalous easterlies.



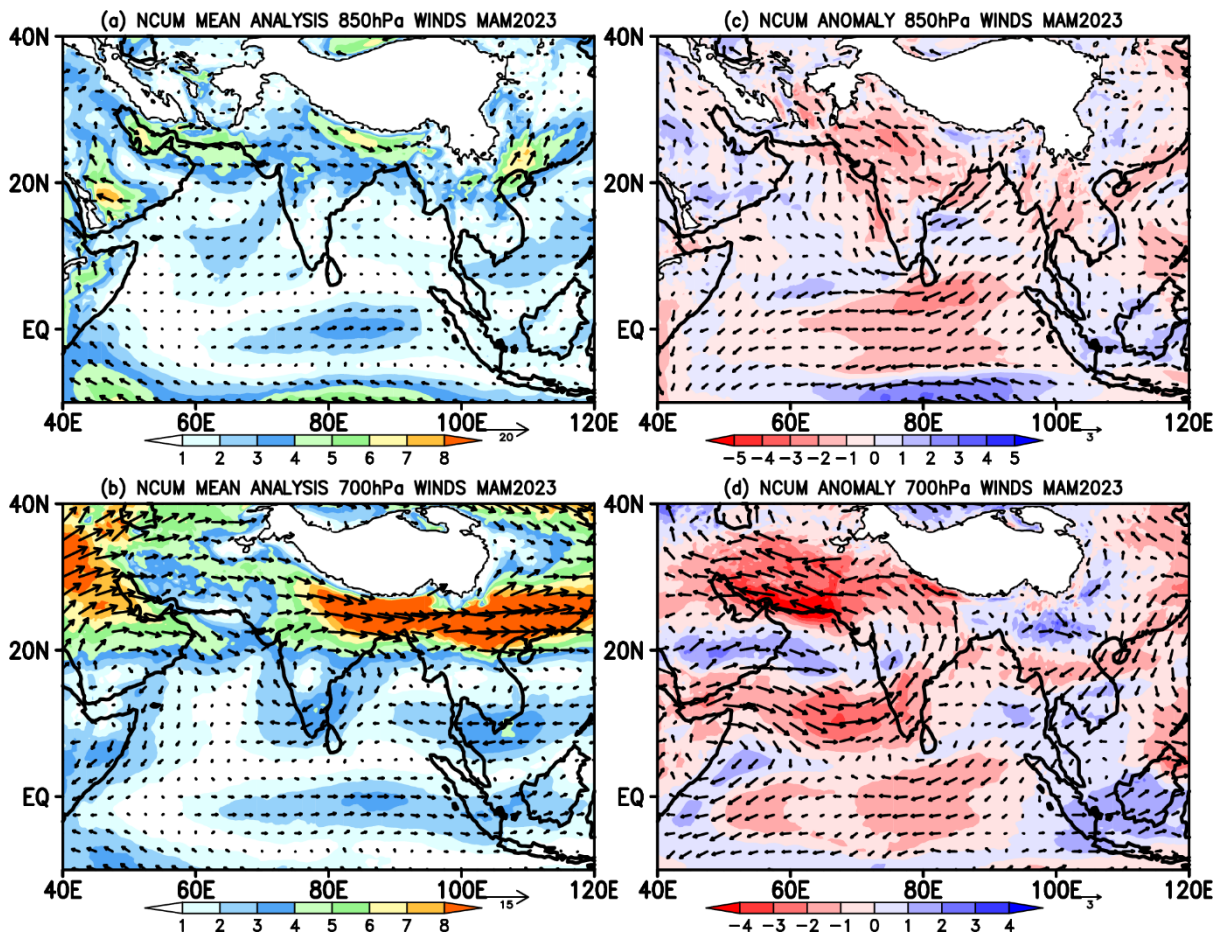


**Figure 1. Mean winds at (a) 850 hPa and (b) 700 hPa in the NCUM-G Analysis during MAM 2023 (m/s). Right panels show the anomaly circulations at (c) 850 hPa and (d) 700 hPa.**

The mean winds from NCUM-G model analysis at 500 hPa and 200 hPa, representative of the mid- and upper troposphere are shown in Figures 2a and 2b, respectively. With increasing altitude, mean winds in the north Indian region enhanced from ~18m/s at 500hPa to more than 40m/s in the upper troposphere. At the same time, winds are relatively weaker in the south Indian region. The associated anomalous winds in the model analysis are shown in Figures 2c and 2d with respect to ERA5 climatology. In the mid- and upper troposphere, the winds exhibit easterlies over northern India and westerlies over the southern peninsular region, consequently creating an anomalous cyclonic circulation clearly visible over the northwestern Indian region (Figures 2c and 2d). In the equatorial regions, the upper tropospheric winds are quite weaker during Pre-monsoon 2023.

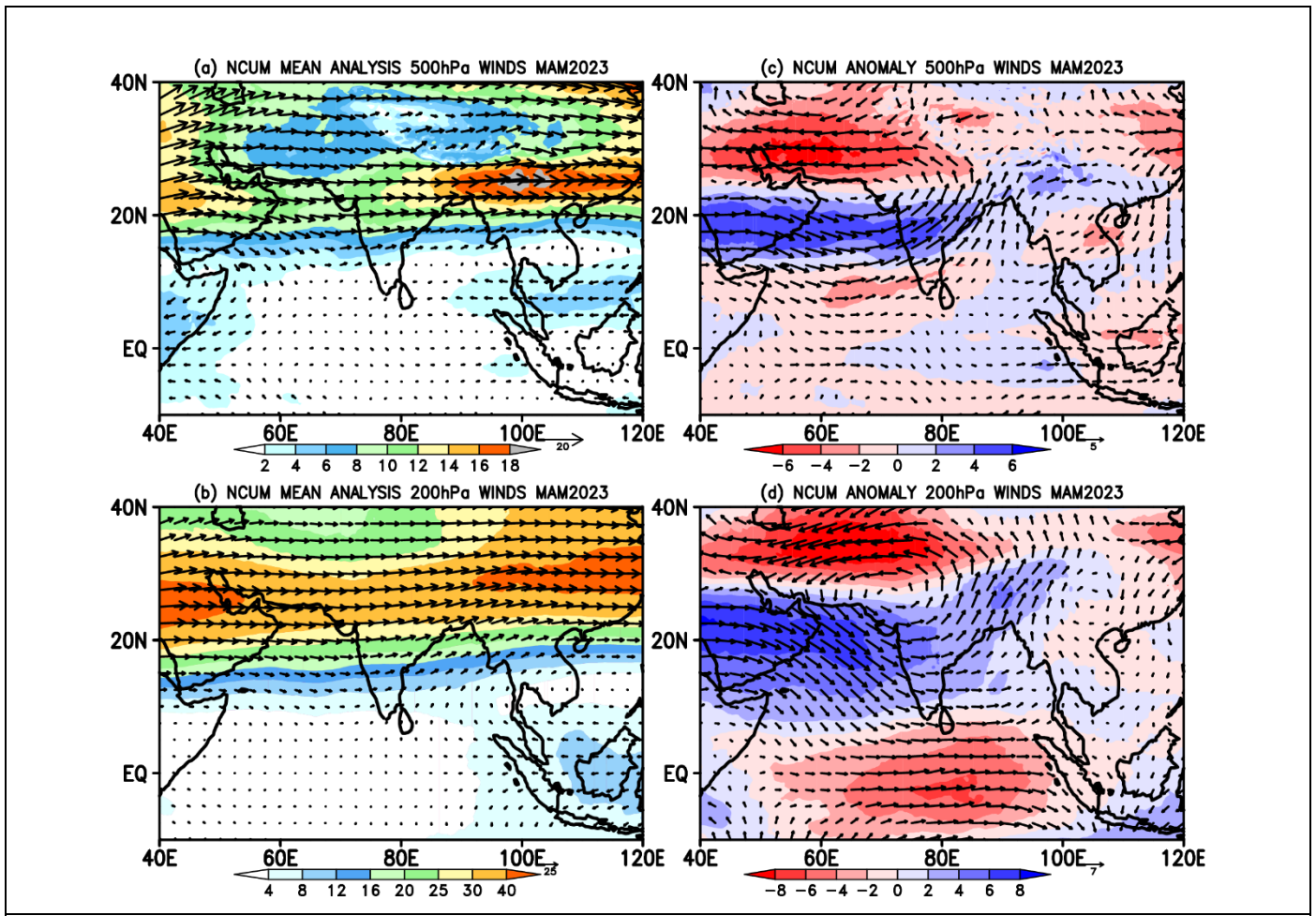


**Figure 2.** Mean winds at (a) 500 hPa and (b) 200 hPa in the NCUM-G Analysis during MAM 2023 (m/s). Right panels show the anomaly circulations at (c) 500 hPa and (d) 200 hPa.

### 3.2. Temperature at 850, 700, 500, and 200 hPa levels

The spatial distribution of seasonal mean temperature is shown in Figure 3. The mean daily temperature at lower levels (i.e., at 850 hPa) exceeds  $20^{\circ}\text{C}$  over the entire Indian region excluding the Indo-Gangetic plains and northern parts of Jammu and Kashmir (Figure 3a). The anomalous temperatures in the lower troposphere (i.e., at 850 hPa and 700 hPa, Figures 3c and 3d) indicate the Pre-monsoon season during 2023 is cooler than the climatology with magnitudes between  $-1^{\circ}$  to  $-2^{\circ}\text{C}$  in the northwest and central parts of India. The cooler temperatures stretch from northwest to southeast India covering the Indo-Gangetic plains. Over the oceans surrounding the Indian subcontinent show warm anomalies with uniform magnitudes  $\sim 1^{\circ}\text{C}$  excluding the northern Arabian Seas (AS). At 200 hPa, the mean temperatures are nearly uniform throughout the Indian subcontinent with local maxima over the Himalayan region (Figure 4c). Nevertheless, the temperature anomalies across India still indicate cooler (warmer) than the climatology at 500 (200) hPa level (Figures 4c and 4d).

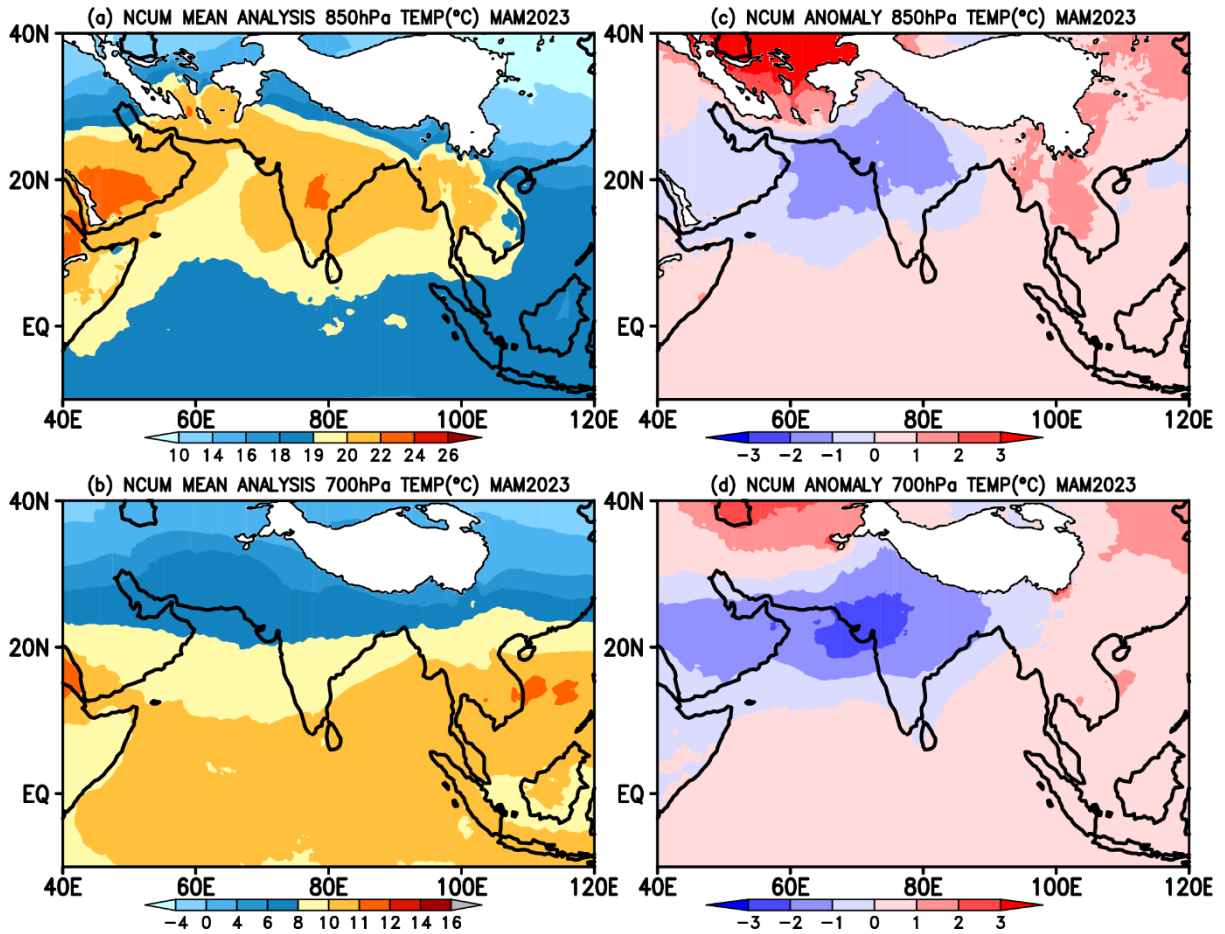
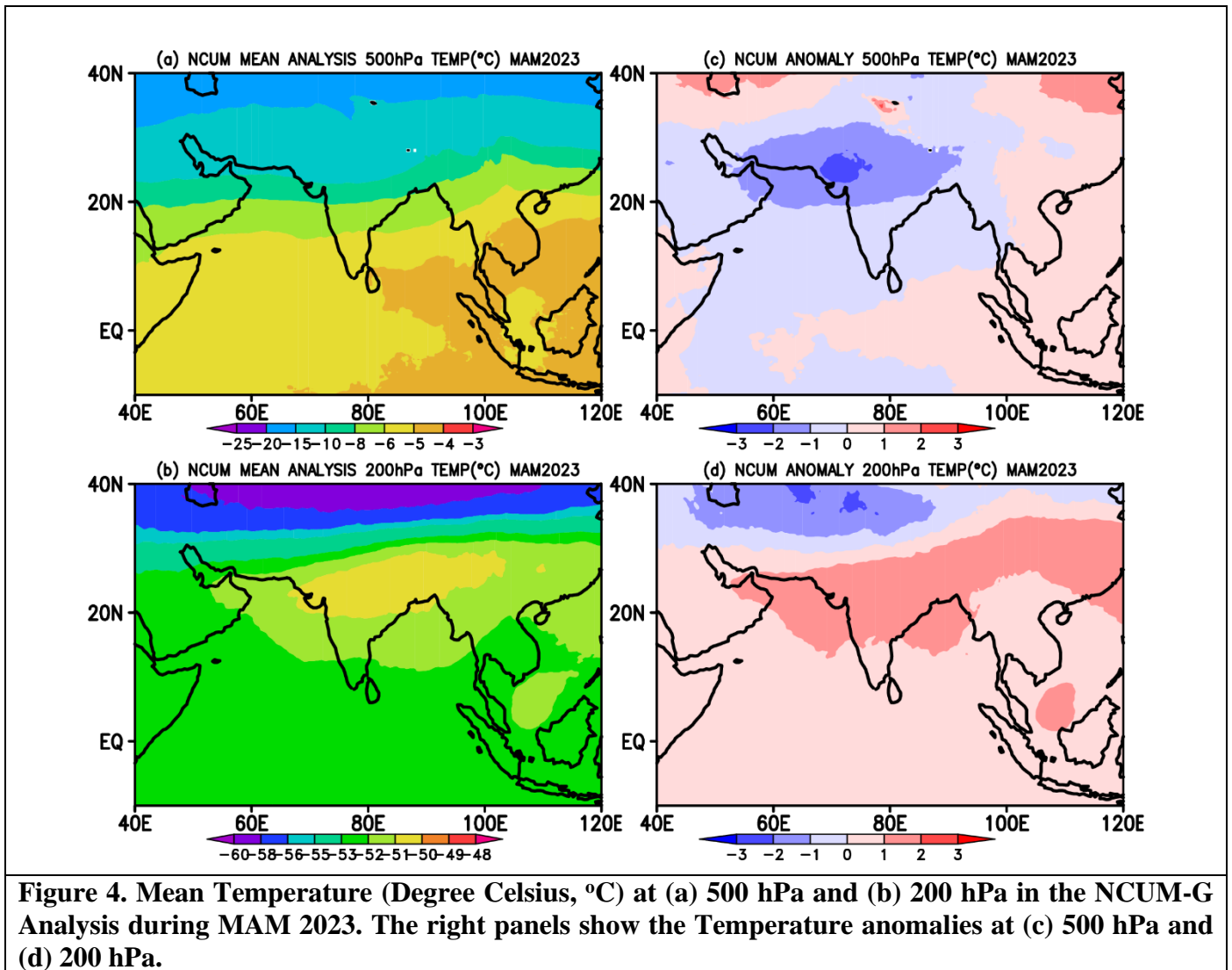


**Figure 3. Mean Temperature (Degree Celsius, °C) at (a) 850 hPa and (b) 700 hPa in the NCUM-G Analysis during MAM 2023. Right panels show the Temperature anomalies at (c) 850 hPa and (d) 700 hPa.**



### 3.3. Relative Humidity (RH) at 850, 700, and 500 hPa levels

The spatial distribution of humidity is an important field along with wind and temperature for its influence on the rainfall. Hence, we further show the spatial distribution of seasonal mean RH from NCUM-G model analysis in Figures 5a (850hPa) and 5b (700hPa). Mean RH at 850 hPa shows higher values over the south relative to north India (Figure 5a). At 700 hPa, the mean RH is found to be higher than 50% over the Indian land region, south of the equator, and around the South China Sea regions (Figure 5b). Also, when we examine the anomalies of MAM 2023 indicates a higher percentage of RH compared to the climatology across India and surrounding oceanic Bay of Bengal (BoB) and AS regions (Figures 5c and 5d). At the same time, negative anomalies are noted in the equatorial regions. These features are also evident in 700 hPa level but with enhanced magnitudes.

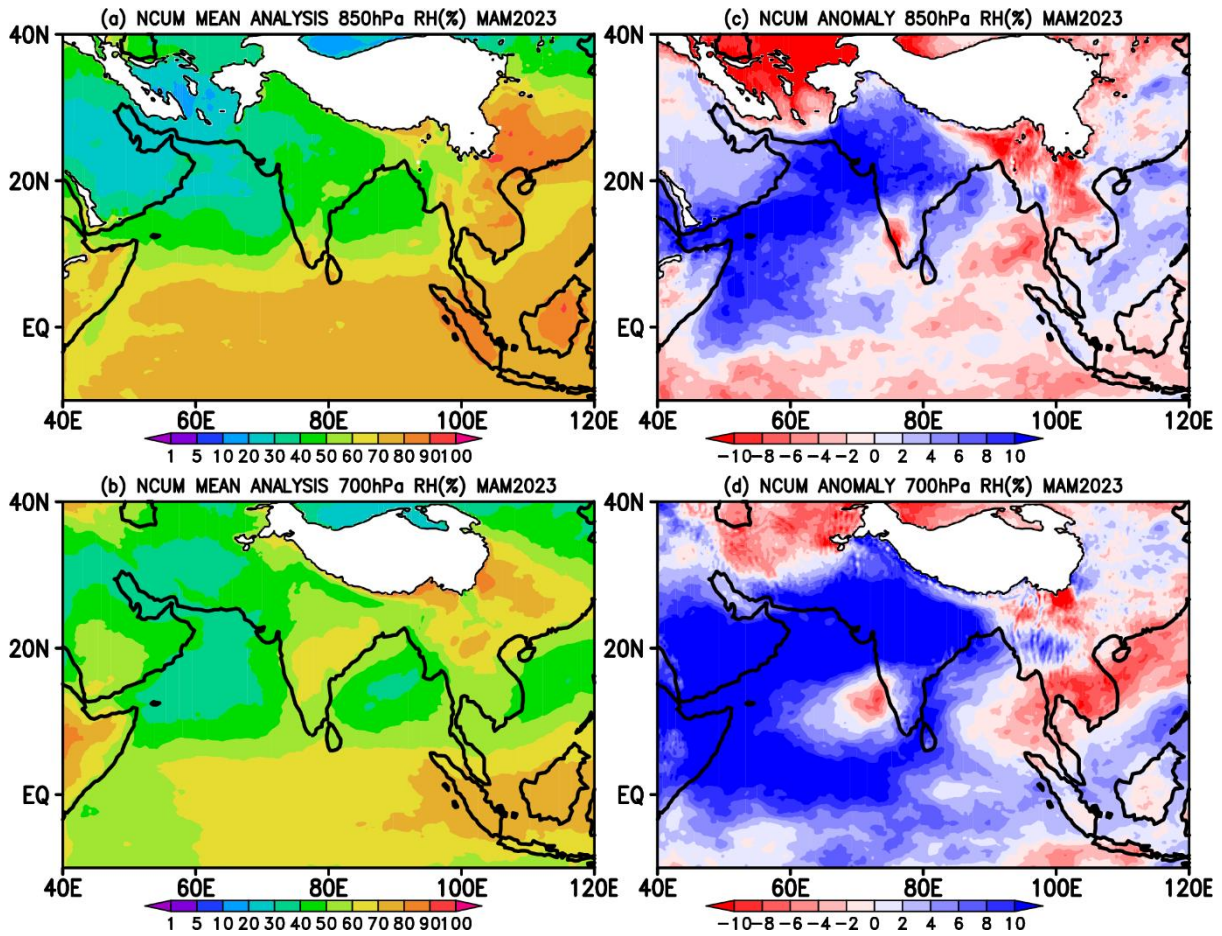


**Figure 5. Mean Relative Humidity (%) at (a) 850 hPa and (b) 700 hPa in the NCUM-G Analysis during MAM 2023. The right panels show the anomalies in Relative Humidity at (c) 850 hPa and (d) 700 hPa.**

Further, we also showed in Figure 6, the spatial distribution of RH in the mid-troposphere at 500 hPa level. The seasonal mean distribution of RH indicates dry conditions over the Indian subcontinent. Nevertheless, occasionally RH can be increased due to the movement of synoptic-scale disturbances in north India during Pre-monsoon. On the other hand, in the oceanic regions, specifically in the maritime continent, a significant amount of the available moisture with RH magnitudes of more than 60% can be noticed (Figure 6a). The anomalous RH distribution is shown in Figure 6 (right panel). The north Indian region shows positive anomalies in RH with respect to climatology, but it may not be significant as the mean RH itself is extremely low. However, negative RH anomalies can be noticed over the maritime continent where the mean distribution is generally higher.

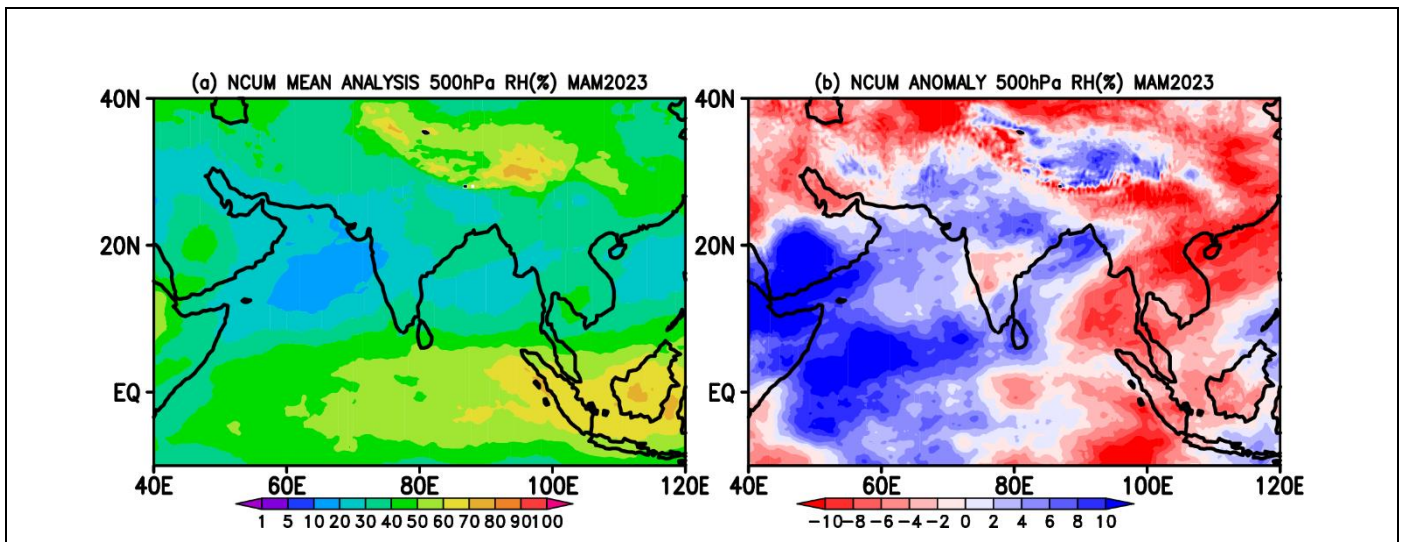


**Figure 6: Mean Relative Humidity (%) at (a) 500 hPa in the NCUM-G Analysis during MAM 2023. The right panel shows the anomalies in Relative Humidity at (b) 500hPa.**

#### 4. Systematic Errors in NCUM-G Forecasts

This section briefly describes systematic errors in the Day-1 (24 hr), Day-3 (72 hr), and Day-5 (120 hr) forecasts during MAM 2023. The forecast errors with respect to model analysis are presented for Winds and Temperature at 850, 700, 500, and 200 hPa levels; and Relative Humidity at 850 and 700 hPa levels (Figure 7-16).

##### 4.1. Winds at 850,700, 500, and 200 hPa levels

Mean winds at 850 hPa level show the presence of ridge-type circulation over central and northwestern Indian regions with prevailing westerly and northwesterly winds. The equatorial regions are also exhibiting mean westerlies with maximum winds reaching ~4m/s (Figure 7a). Systematic errors in winds from Day-1 forecasts at this level show a westerly wind bias over the northern Indian region and along the west coast. Enhanced north westerlies are more prominent along the west coast. The errors are consistent with forecast lead times but with enhanced magnitudes during pre-monsoon season (Figures 7a-d). Similar systematic errors in winds are also noticed at 700 hPa level over the Indian region. In addition, westerly wind bias is more prominent at 700 hPa level over the eastern equatorial Indian Ocean in Day-3 and Day-5 forecasts (Figures 8c-d).

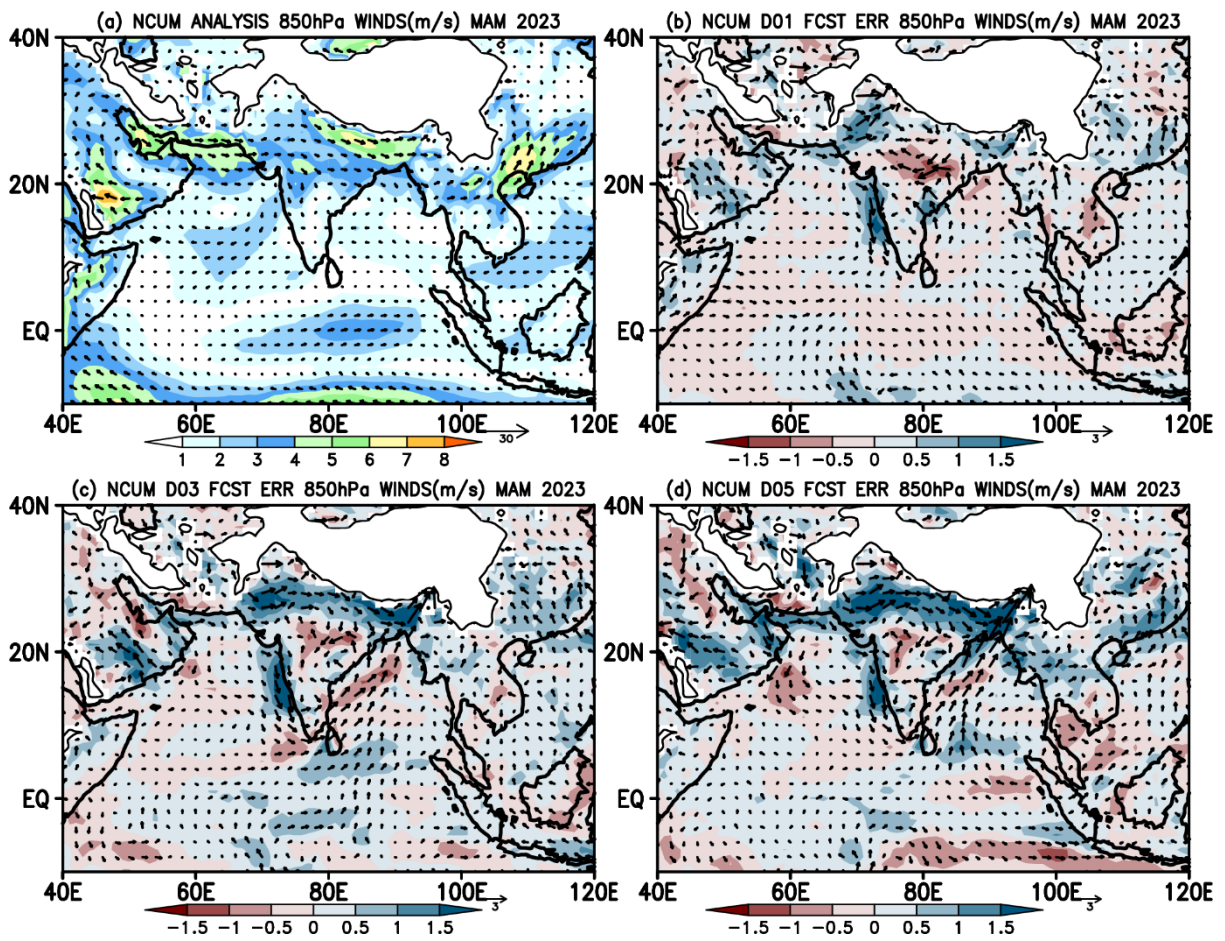


**Figure 7. (a) Mean winds (m/s) and systematic errors (m/s) in (b) Day-1, (c) Day-3, and (d) Day-5 forecasts at 850 hPa during MAM 2023.**

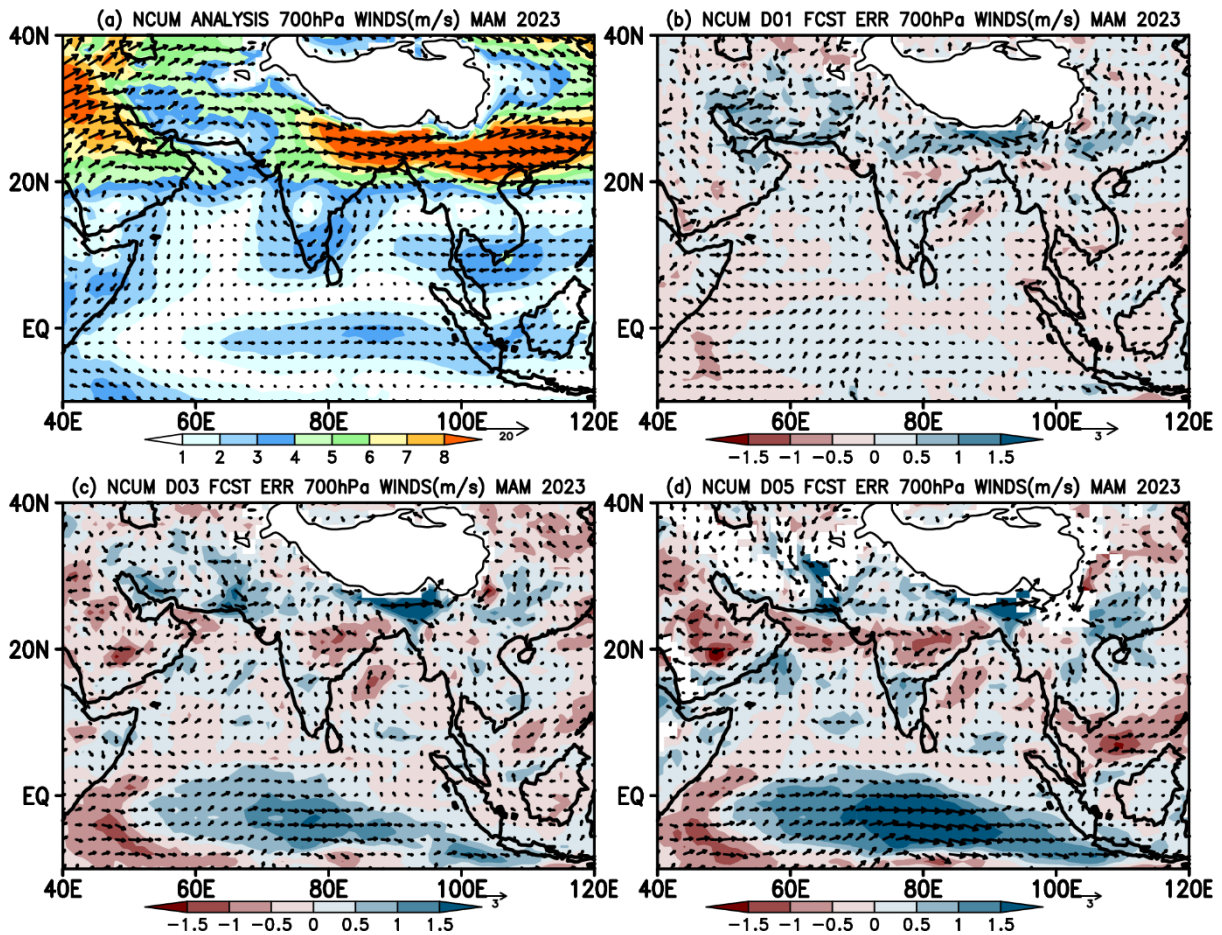


**Figure 8. (a) Mean winds (m/s) and systematic errors (m/s) in (b) Day-1, (c) Day-3, and (d) Day-5 forecasts at 700 hPa during MAM 2023.**

Mean winds at 500 hPa level show strong westerlies between 30-40° N and these westerly winds penetrated over the north and central Indian region (Figure 9a). Errors in winds at 500hPa level are relatively small in Day-1 forecasts. The south-easterly wind bias seen over most of the Indian land mass and the westerly wind bias over the western equatorial Indian Ocean seems enhancing in Day-3 and Day-5 forecasts. The enhanced westerlies exhibit cyclonic circulation just above the equator in Day-5 forecast around 500 hPa level, which is noteworthy (Figures 9a-d). Systematic errors at 200 hPa level winds show enhanced divergent circulation centered around central parts of India as seen in Day-3 forecasts and a similar spatial pattern in winds is also seen in Day-5 forecasts with enhanced error magnitudes (Figure 10 c-d).



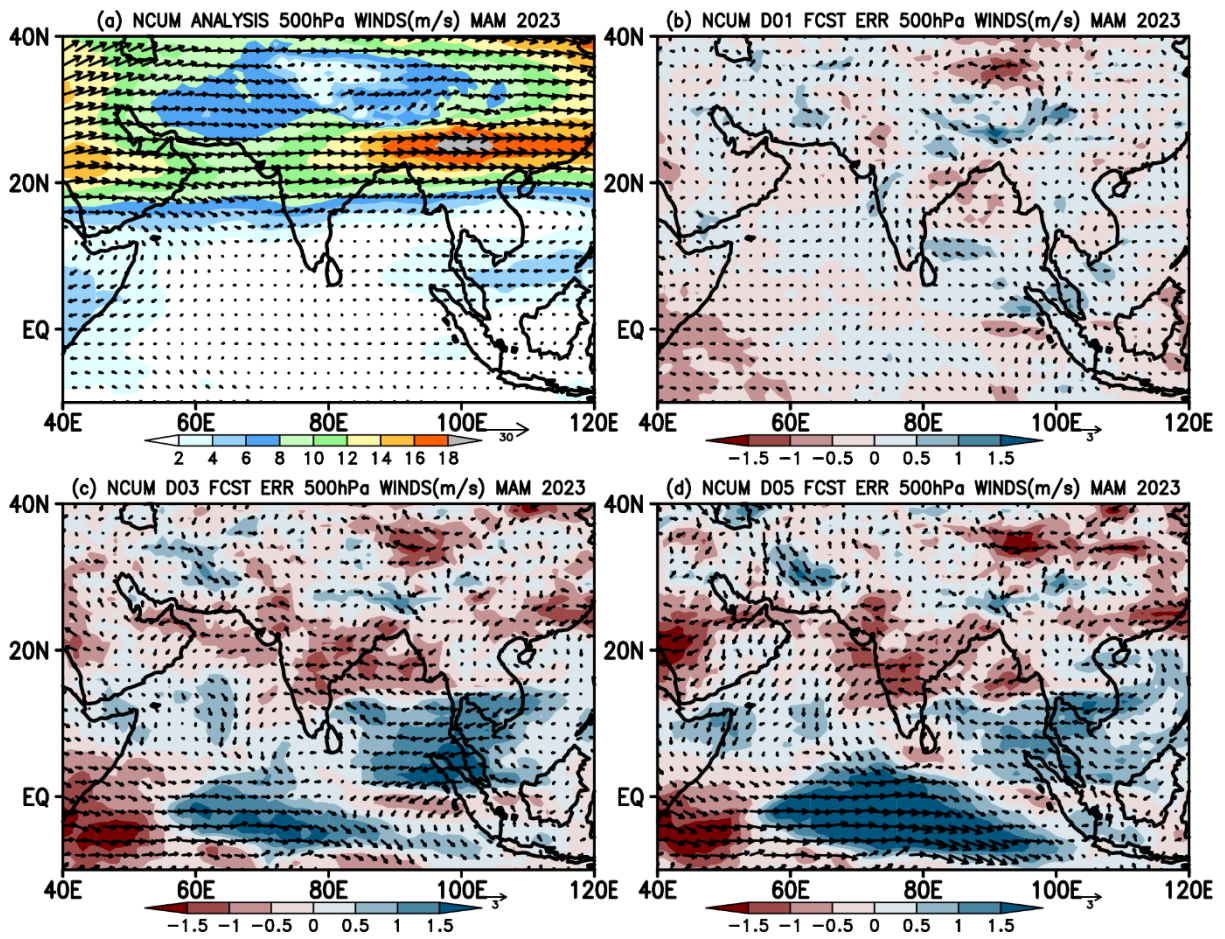


**Figure 9. (a) Mean winds (m/s) and systematic errors (m/s) in (b) Day-1, (c) Day-3, and (d) Day-5 forecasts at 500 hPa during MAM 2023.**

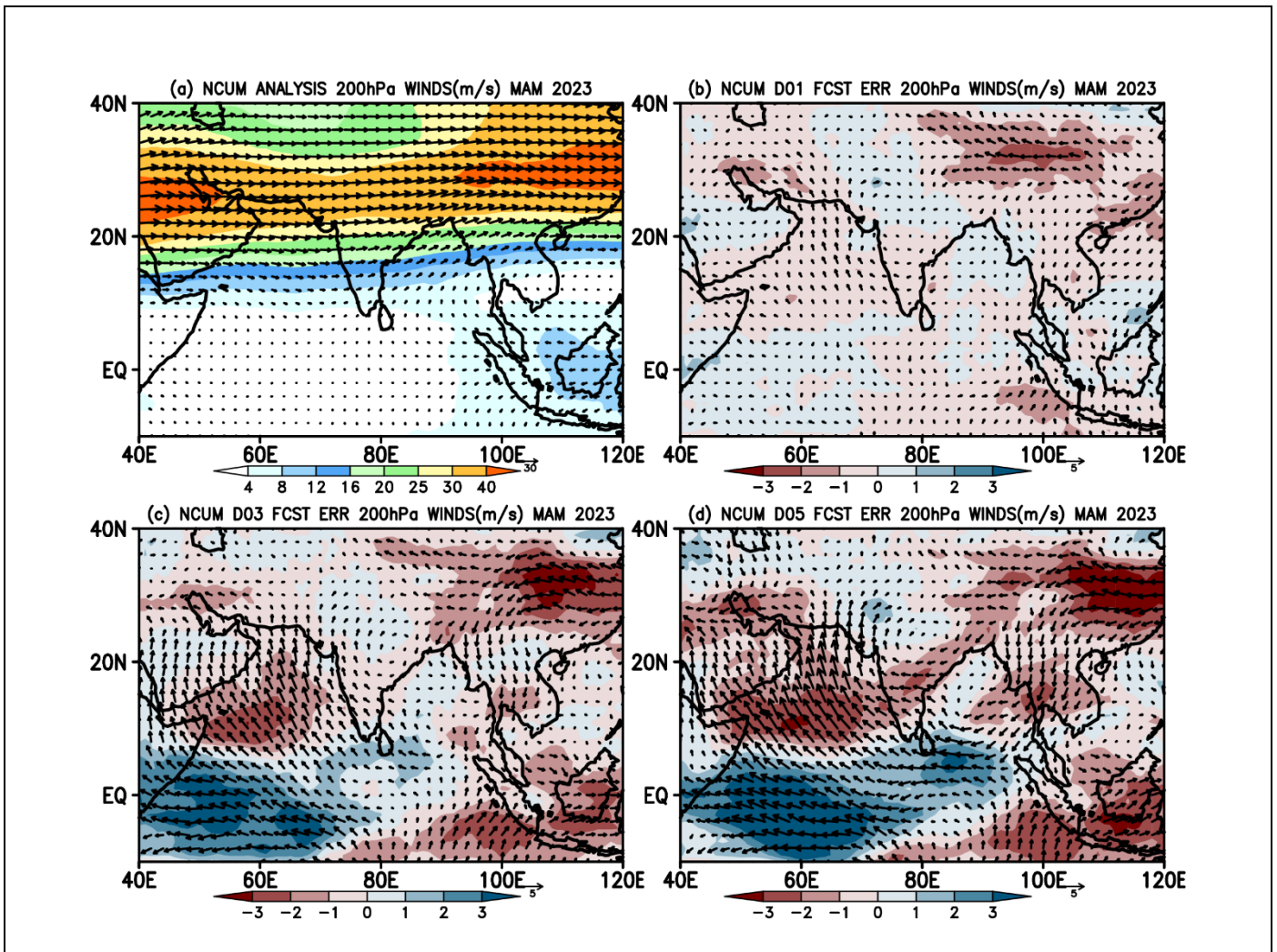


**Figure 10. (a) Mean winds (m/s) and systematic errors (m/s) in (b) Day-1, (c) Day-3, and (d) Day-5 forecasts at 200 hPa during MAM 2023.**

## 4.2. Temperature and Relative humidity

Spatial map of seasonal mean temperature from NCUM-G analysis at 850 hPa shows relatively warm temperatures (19-22°C) over BoB and AS (Figure 11a). The model shows warm bias ranging from ~1-3°C occupied over most of the Indian land mass and the magnitude of this bias is increasing with forecasts lead time (Figures 11 b-d). These error increments at 850 hPa temperatures are also more prominent over the Indo-Gangetic plain (IGP) regions. On a similar note, the temperature at 700 hPa (Figure 12) also shows warm bias (>1°C) over most of the Indian land region. It is interesting to see that the bias over the south Arabian Sea (AS) reverse sign and now exhibits warm bias compared to the 850h Pa level. This warm bias over south AS is also seen in Day-3 and Day-5 forecasts. The BoB region also exhibits slight warming in all the forecast days, i.e., from Day-1 to Day-5 (Figures 12 b-d). At 500 hPa (200 hPa) level, temperature exhibits warm (cold) bias over the Indian land region including surrounding oceanic regions, and the magnitude of the bias

is increasing in forecasts with lead time (Figures 13 b-d (Figures 14 b-d)). Furthermore, a warm bias is observed at 500 hPa over the western Arabian Sea and the adjacent region, as well as at 200 hPa over northwestern India and the adjoining area in Day-3 forecasts. This bias becomes more pronounced in Day-5 forecasts (Figures 13 b-d and Figures 14 b-d).

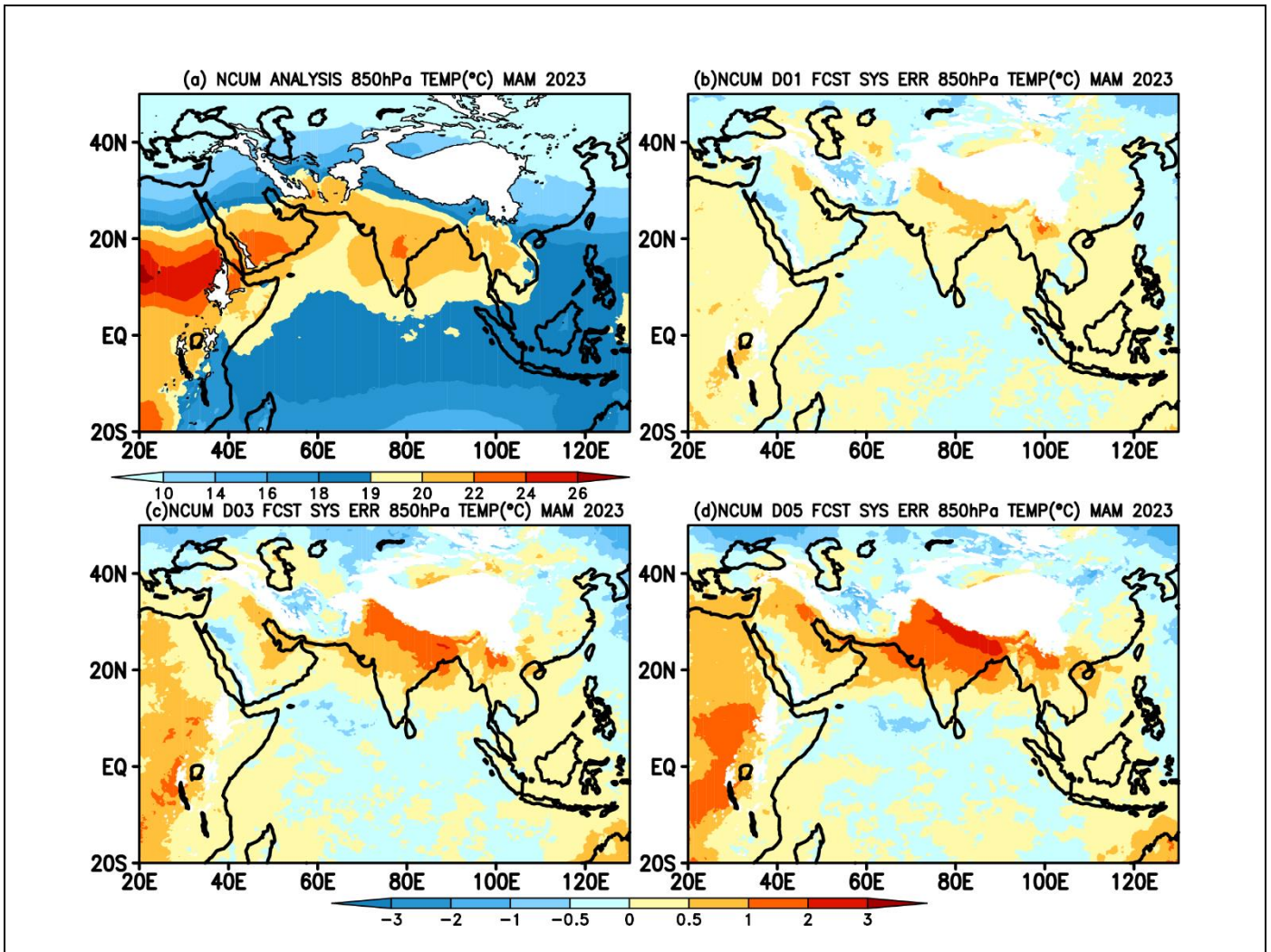


**Figure 11. (a) Mean Temperature (Degree Celsius, °C) and systematic errors (Degree Celsius, °C) in (b) Day-1, (c) Day-3, and (d) Day-5 forecasts at 850 hPa during MAM 2023.**

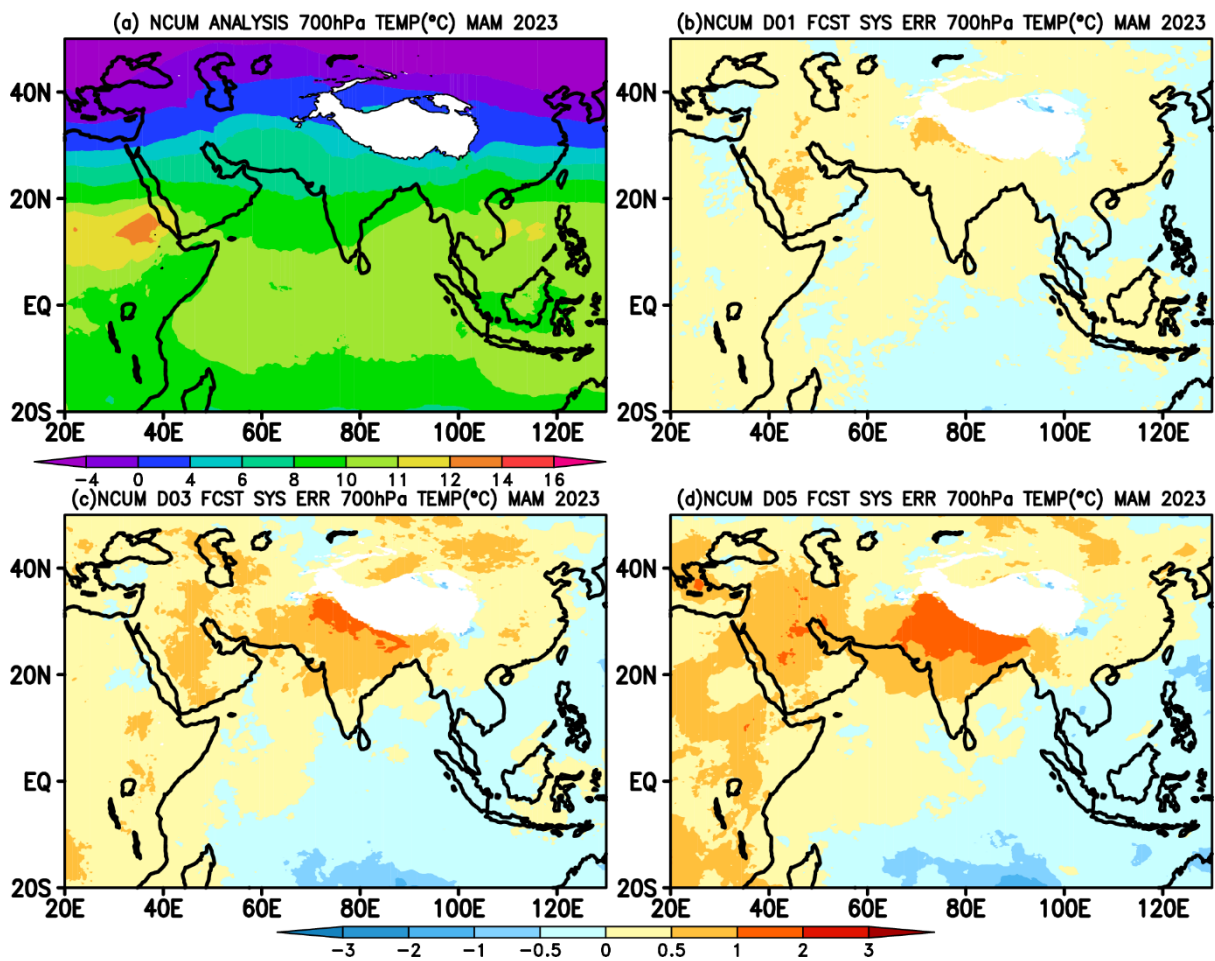


**Figure 12. (a) Mean Temperature (Degree Celsius, °C) and systematic errors (Degree Celsius, °C) in (b) Day-1, (c) Day-3, and (d) Day-5 forecasts at 700 hPa during MAM 2023.**

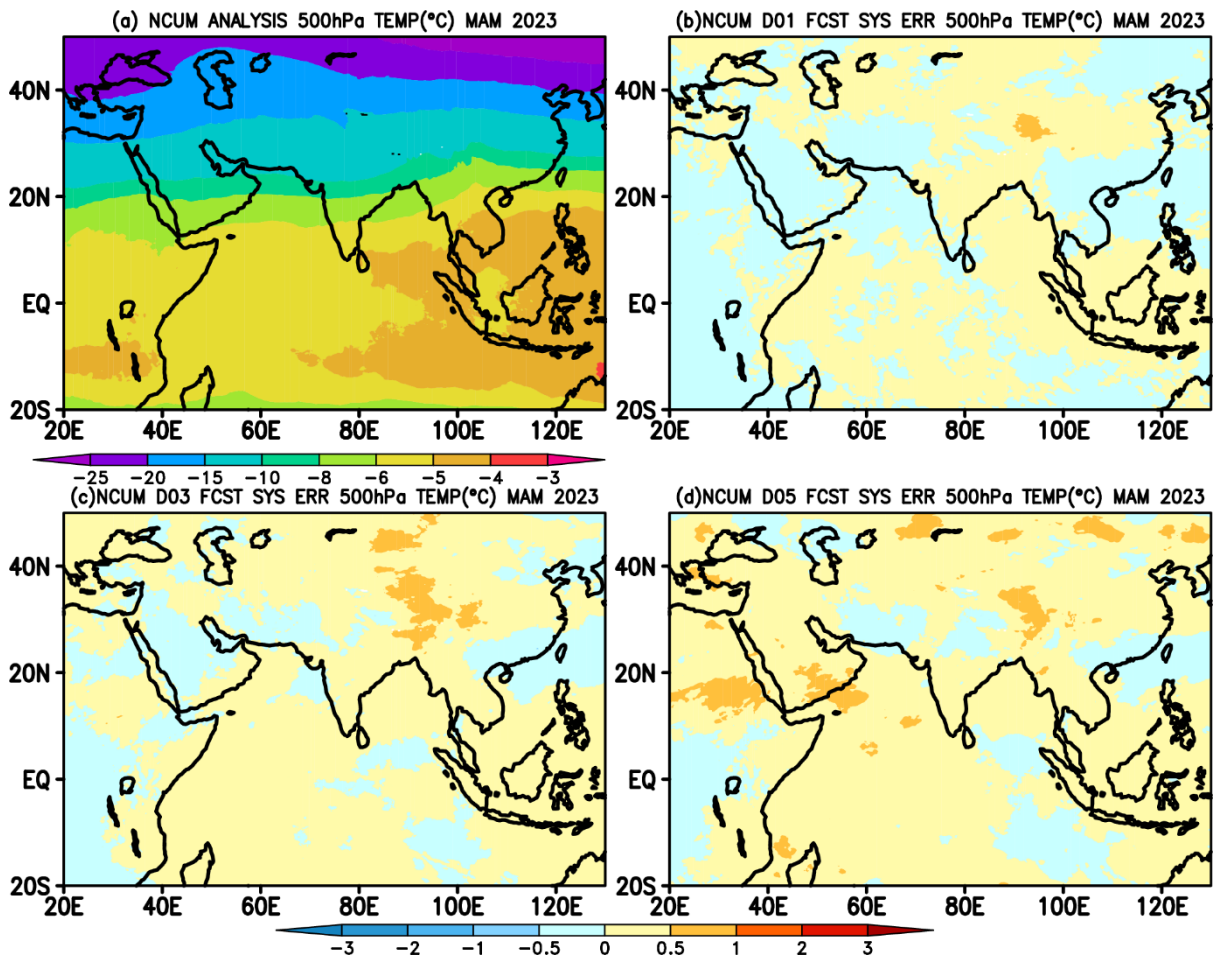


**Figure 13. (a) Mean Temperature (Degree Celsius, °C) and systematic errors (Degree Celsius, °C) in (b) Day-1, (c) Day-3, and (d) Day-5 forecasts at 500 hPa during MAM 2023.**

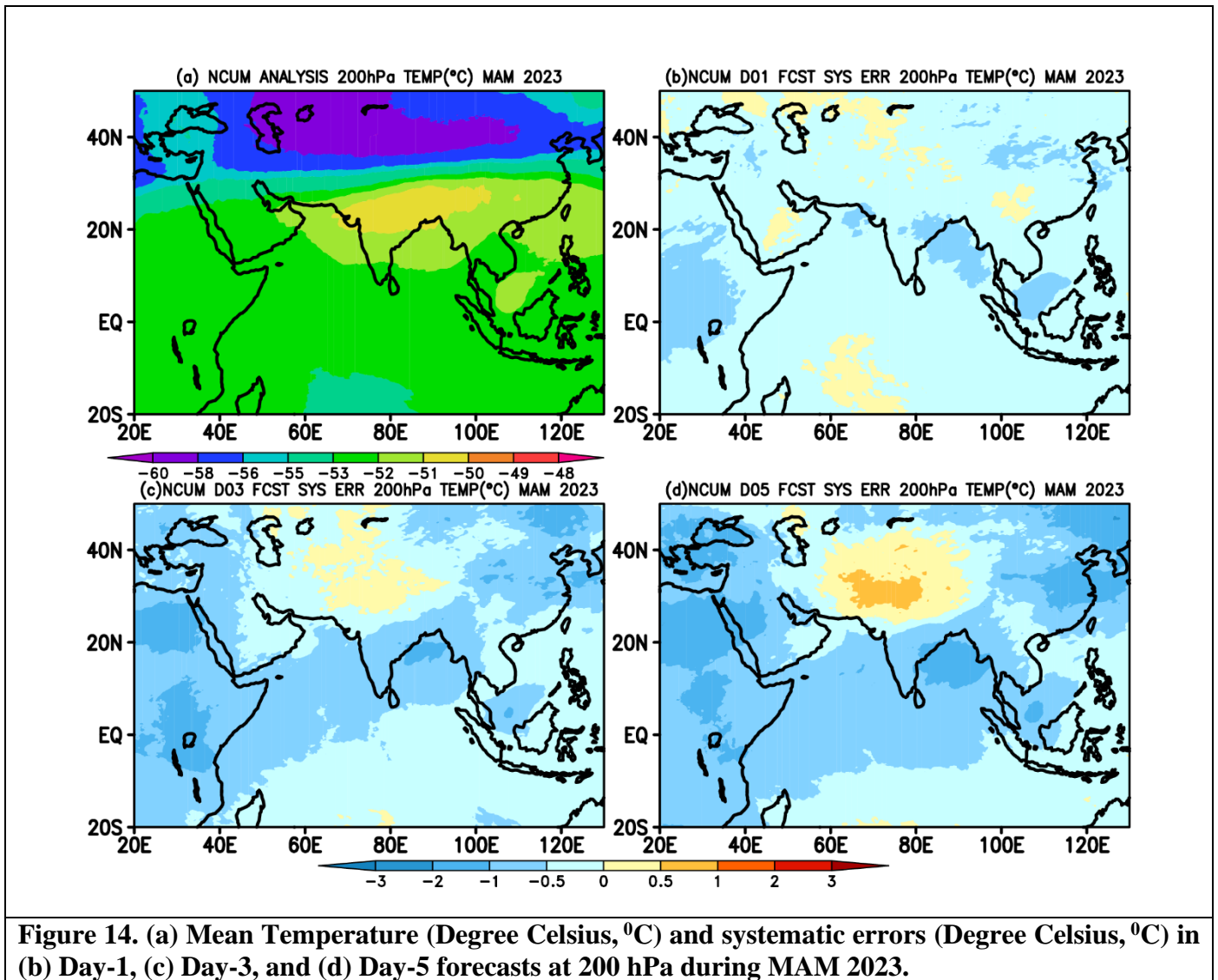


**Figure 14. (a) Mean Temperature (Degree Celsius, °C) and systematic errors (Degree Celsius, °C) in (b) Day-1, (c) Day-3, and (d) Day-5 forecasts at 200 hPa during MAM 2023.**

Seasonal mean RH at 850 (Figure 15) and at 700 hPa (Figure 16) levels show large values > 80% over the south of the equator and around South China Sea regions, and relatively lower RH values over Northern parts of the Indian subcontinent. Systematic errors show a large dry bias over Indian land regions at 850 hPa level, and this dryness is enhancing with forecasts lead time (Figures 15 c-d). The presence of low-level anticyclone over the Indian sub-continent induces enhanced warming, which could be one primary reason for the negative RH values over the central Indian region (Figures 15c-d). On the contrary, oceanic regions exhibit moist bias as evidenced by positive RH values, except Africa and West Arabian regions. Interestingly the moist bias observed over the oceanic regions (i.e., AS and BoB) at 850 hPa level change sign to negative, and dry bias is seen at 700 hPa level. Additionally, the moist bias south of the equator is getting intensified in the Day-3 and Day-5 forecast and the entire column is occupied with excess moisture at 700 hPa levels (Figures 16 b-d).

In the next section, a brief description of systematic errors in the model forecasts is presented for key surface variables such as 2m Temperature (Figure 17), 10m Winds (Figure 18), and Total Precipitable water (PWAT; Figure 19). The errors are computed against the NCUM-G analysis.

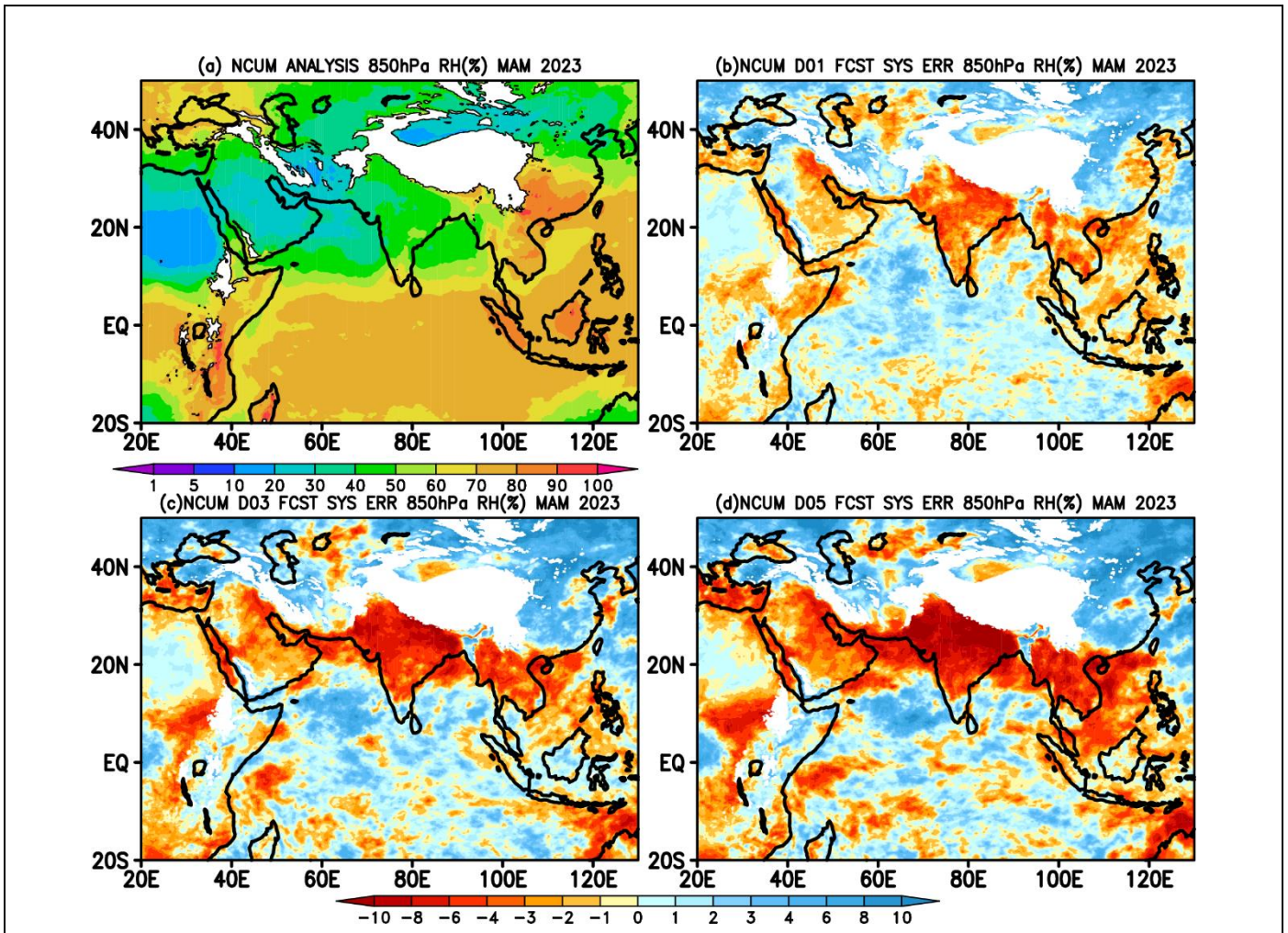


**Figure 15. (a) Mean Relative Humidity (%) and systematic errors (%) in (b) Day-1, (c) Day-3, and (d) Day-5 forecasts at 850 hPa during MAM 2023.**

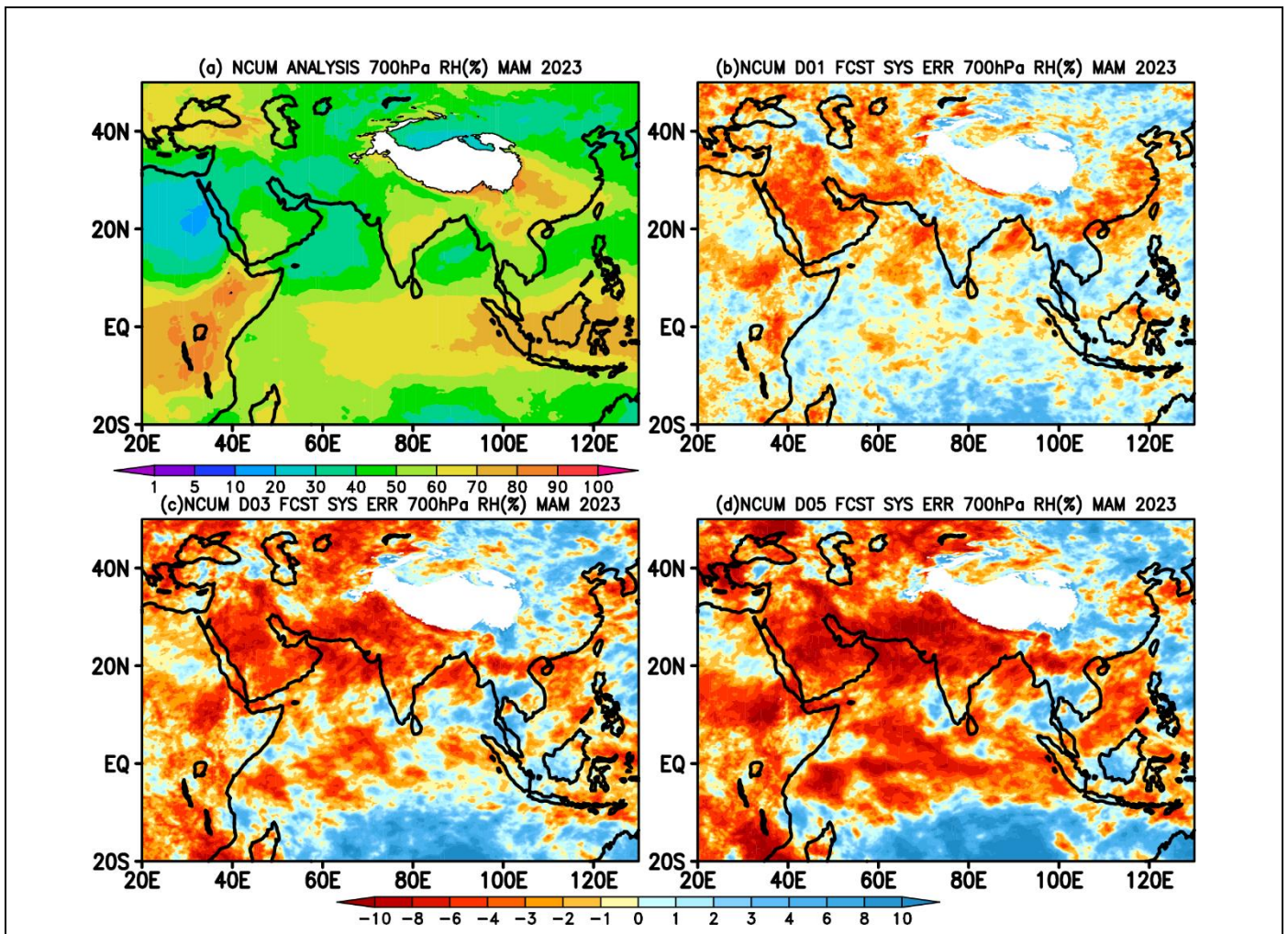


**Figure 16. (a) Mean Relative Humidity (%) and systematic errors (%) in (b) Day-1, (c) Day-3, and (d) Day-5 forecasts at 700 hPa during MAM 2023.**

### 4.3. Surface (10m) winds

Seasonal mean winds at 10m from the analysis show the presence of relatively strong north-westerlies over the AS, south-westerlies over head Bay of Bengal (BoB), and weak westerlies over the tropical Indian Ocean (TIO) while strong easterlies south of TIO around 80°E. The systematic errors in the forecasts depict a few notable features; 1) The north-westerly wind bias along the west coast over the northern AS and south-westerly wind bias along the east coast over BoB in Day-1 forecast is enhancing its strength with forecast lead time. 2) On a similar note, the easterly wind biases seen in the Day-1 forecast around the equator and south of the equator close to the maritime continent are also getting intensified in the Day-5 forecast (Figures 17 b-d).



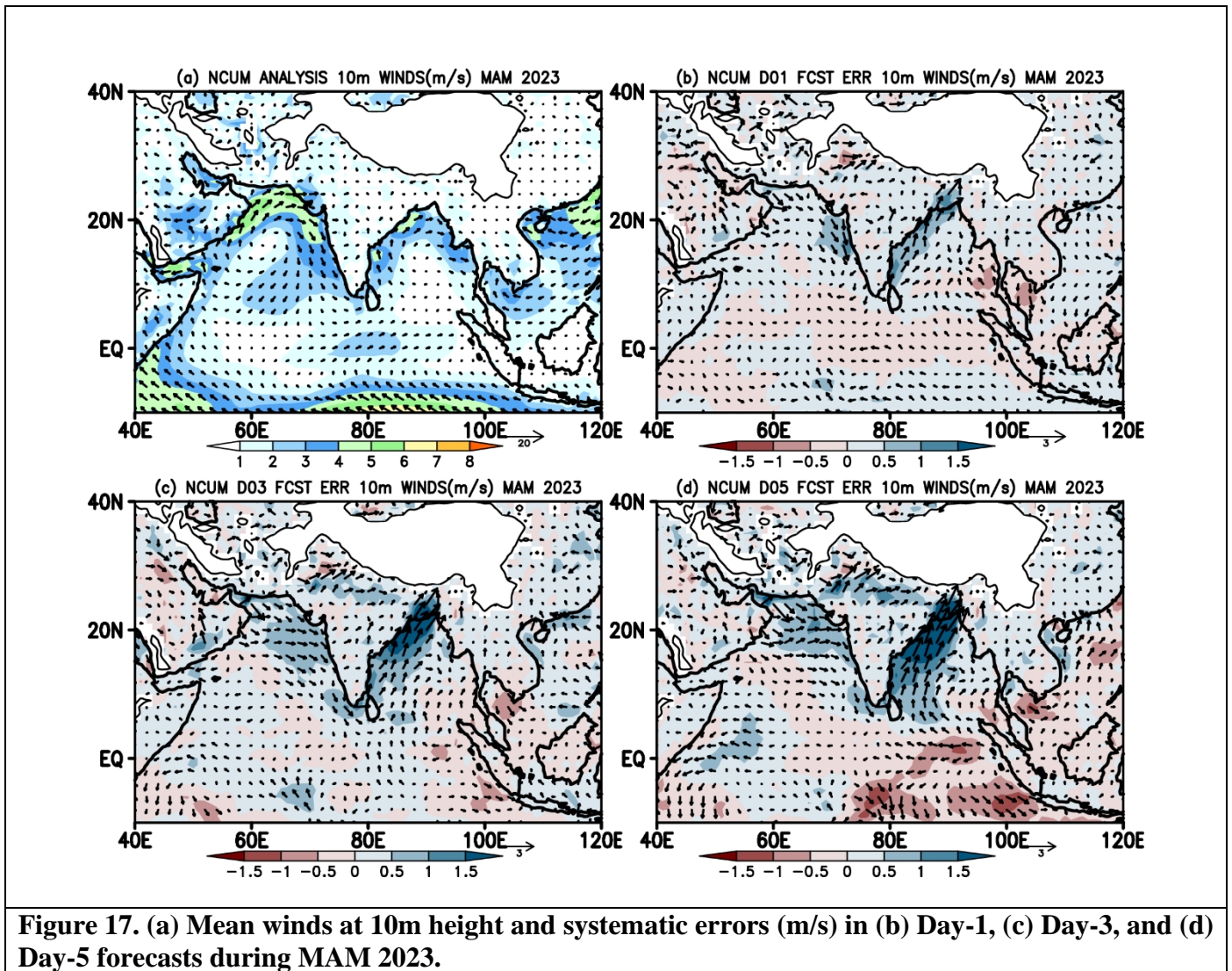


**Figure 17. (a) Mean winds at 10m height and systematic errors (m/s) in (b) Day-1, (c) Day-3, and (d) Day-5 forecasts during MAM 2023.**

#### 4.4. Temperature at 2m

Seasonal temperature patterns over the Indian region show warm temperatures (33-40<sup>0</sup>C) on the Indian land mass and relatively cold temperatures over oceanic regions (Figure 18a). Systematic errors show a relatively warm bias over the Indian land regions. Interestingly this warm bias is increasing with forecast lead time. This can be attributed to the dry north-westerly winds from the northwest entering Indian land and north AS (Figures 18 c-d). In addition, most of the oceanic regions of BoB and AS exhibited cold bias of the range < -0.5<sup>0</sup>C in all the forecast times. In addition, model temperature also exhibits a warm bias over the west of AS. It is noted that the magnitude of the bias is increasing with forecast lead time, which is noteworthy (Figures 18 c-d).

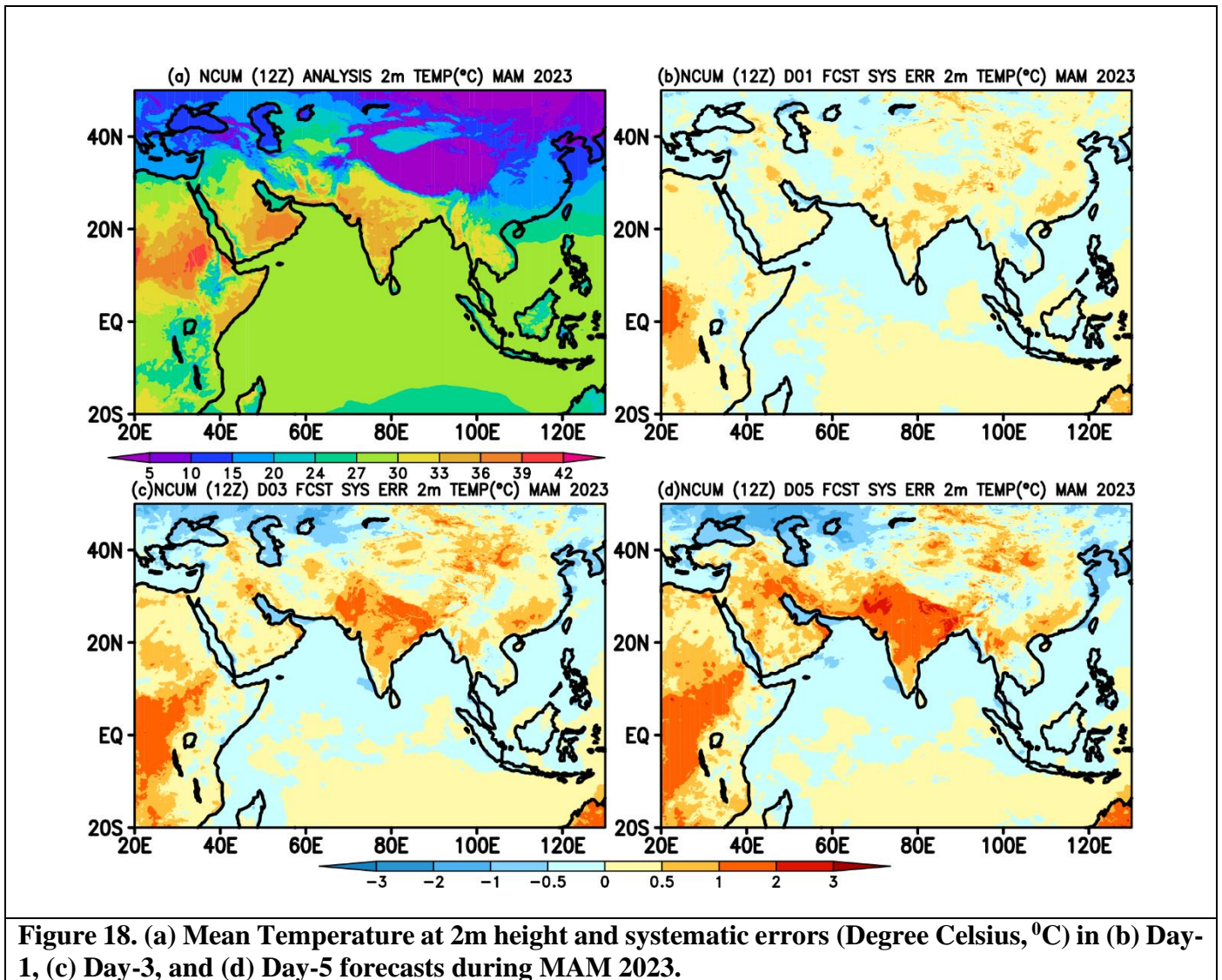
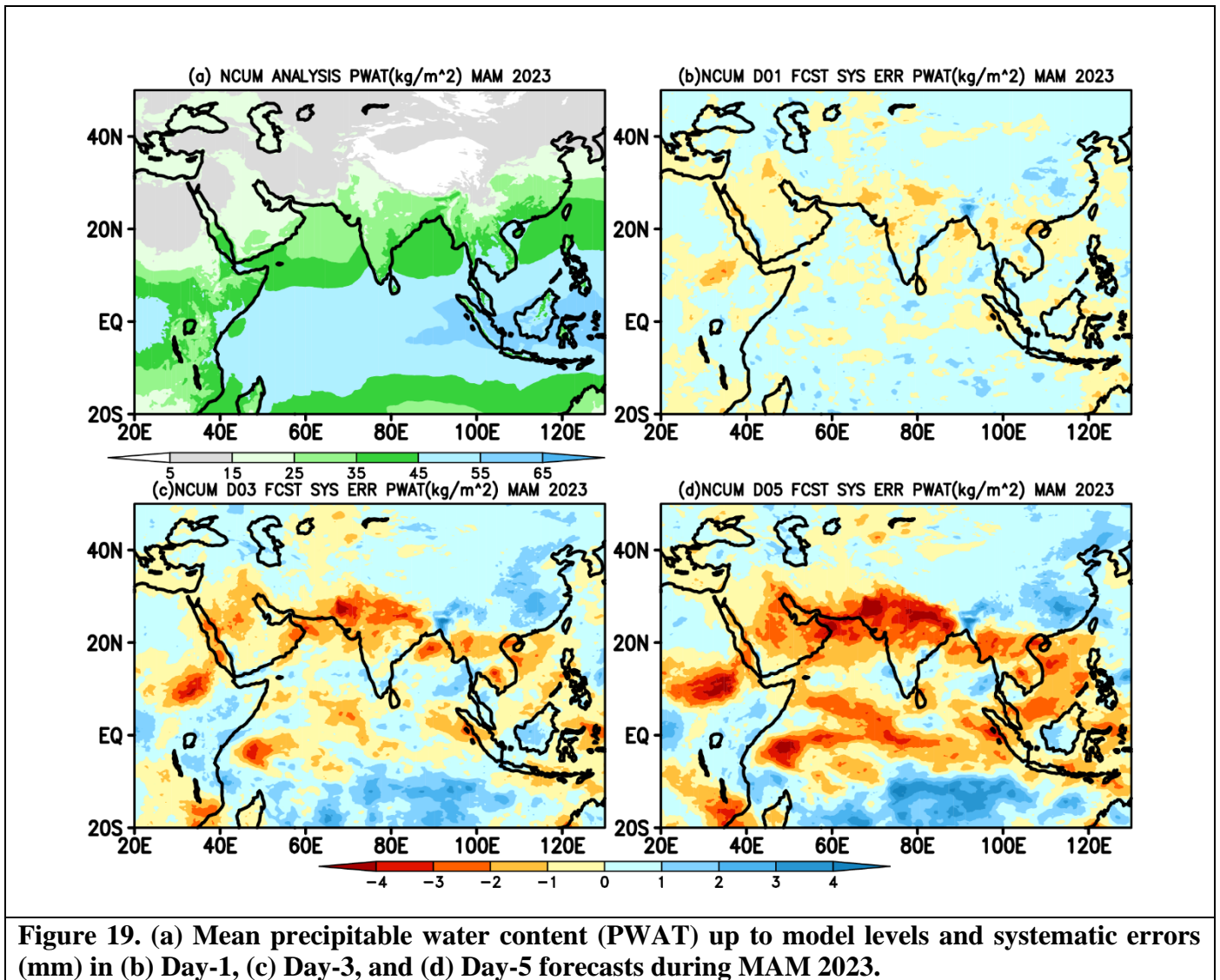


**Figure 18. (a) Mean Temperature at 2m height and systematic errors (Degree Celsius, °C) in (b) Day-1, (c) Day-3, and (d) Day-5 forecasts during MAM 2023.**

#### 4.5. Total Precipitable Water (PWAT)

Seasonal mean PWAT shows a large value ( $> 60$  mm) around the equatorial regions, especially over the Maritime Continent (MC) owing to the presence of a warm pool and associated convection during the pre-monsoon season over these regions. In contrast, most of the northern and central Indian regions are dry with very less PWAT values (5-25 mm). However, extreme southeast peninsular India exhibits moderate PWAT values around 35-40 mm due to the westerly winds from the MC region (Figure 19a). Systematic error in PWAT shows a column dry over Indian land regions in the Day-1 forecast, this dryness in column is enhancing with forecast lead time and its magnitude is maximum in the Day-5 forecast (Figures 19 c-d). Moderately positive PWAT bias is seen over the south of equatorial regions. This excess column water could be one reason for excess rainfall in this region.



## 5. Forecast Verification during MAM 2023

Verification of NCUM-G model rainfall forecasts is presented in this section for MAM 2023. The daily accumulated rainfall forecasts are verified against the NCMRWF-IMD merged satellite and gauge rainfall product. The discussion presented in this section is confined to mean and mean error (ME) over the India region. Further, this section also quantifies forecast skill using standard verification metrics, namely, the probability of detection (POD), false alarm ratio (FAR), and critical success index (CSI) which are described in standard textbooks (Wilks, 2011, Jolliffe and Stephenson, 2012); and Symmetric extremal dependence index (SEDI), a metric for extreme and rare events (Stephenson et al 2008, Ashrit et al 2015b, Sharma et al 2021).

### **5.1. Rainfall Mean and Mean Error**

The observed and forecast mean rainfall during MAM 2023 is shown in Figure 20. Observations indicate that most of the Indian subcontinent is dry in this season. However, we can notice the rainfall amounts over the northern parts of India that are associated with the disturbances/troughs approached from the west which are usually termed western disturbances (WDs). Moderate rainfall (2-4 mm/day) is also seen over southern parts of peninsular India, along the eastern coast, and the north-eastern regions (Figure 20a). The panels in the middle row, Figures 20 b-d show the Day-1, Day-3, and Day-5 NCUM-G forecast rainfall averaged during the MAM2023 period. The observed rainfall regions are well predicted in all the forecast times. However, it is found that the NCUM-G forecast overestimates rainfall amounts over central India, along the eastern coast, and the north-eastern regions. Apart from this most of the Indian subcontinent is dry with no convection in both observations and forecasts (Figures 20 a-d). Now, to further quantification forecast mean errors (ME) are computed against the observation. The panels in the bottom row show rainfall ME (Figures 20 e-g) in predicted rainfall indicating wet bias (blue) over north-eastern parts while dry bias off-coast of Odisha, Andhra Pradesh, Tamil Nādu, and Myanmar regions, and the magnitude of dry bias is increases with lead time.

### **5.2. Categorical Scores of Rainfall Forecasts**

To further quantify the model rainfall forecasts, categorical skill scores are computed over the Indian subcontinent. The categorical approach of verifying quantitative precipitation forecast (QPF) is generally based on the 2 x 2 contingency table which is evaluated for each threshold. Verification scores are presented for rainfall of up to 30mm/day. For different rainfall thresholds, the probability of detection (POD) and the false alarm ratio (FAR) show a decrease and increase in scores, respectively. The BIAS score (frequency bias) indicates that forecasts overestimate the frequency at various thresholds. The values of the Peirce's skill score (PSS) and the Symmetric extremal dependence index (SEDI), all are high for rainfall up to 3-6 mm/day suggesting reasonable skill. PSS score shows a very sharp decrease as the threshold varies. Overall, the skill is not bias-free. For higher rainfall thresholds (> 10 mm/day), frequency bias is almost constant, but the skill is low as indicated by the critical success index (CSI), PSS, and SEDI (Figure 21).

### **5.3. Categorical Scores of $T_{max}$**

Similar analysis as discussed in the above section is repeated for maximum temperature thresholds. The POD slightly increases with the thresholds from 30<sup>0</sup>C to 44<sup>0</sup>C while the PSS score is nearly constant and below 0.3 till 40 <sup>0</sup>C, thereafter it slightly increases to above 0.3. FAR scores over all India as whole show relatively

large values  $>0.6$  in all temperature thresholds and varies between 0.6-0.8 in all forecast lead times (Figure 22).

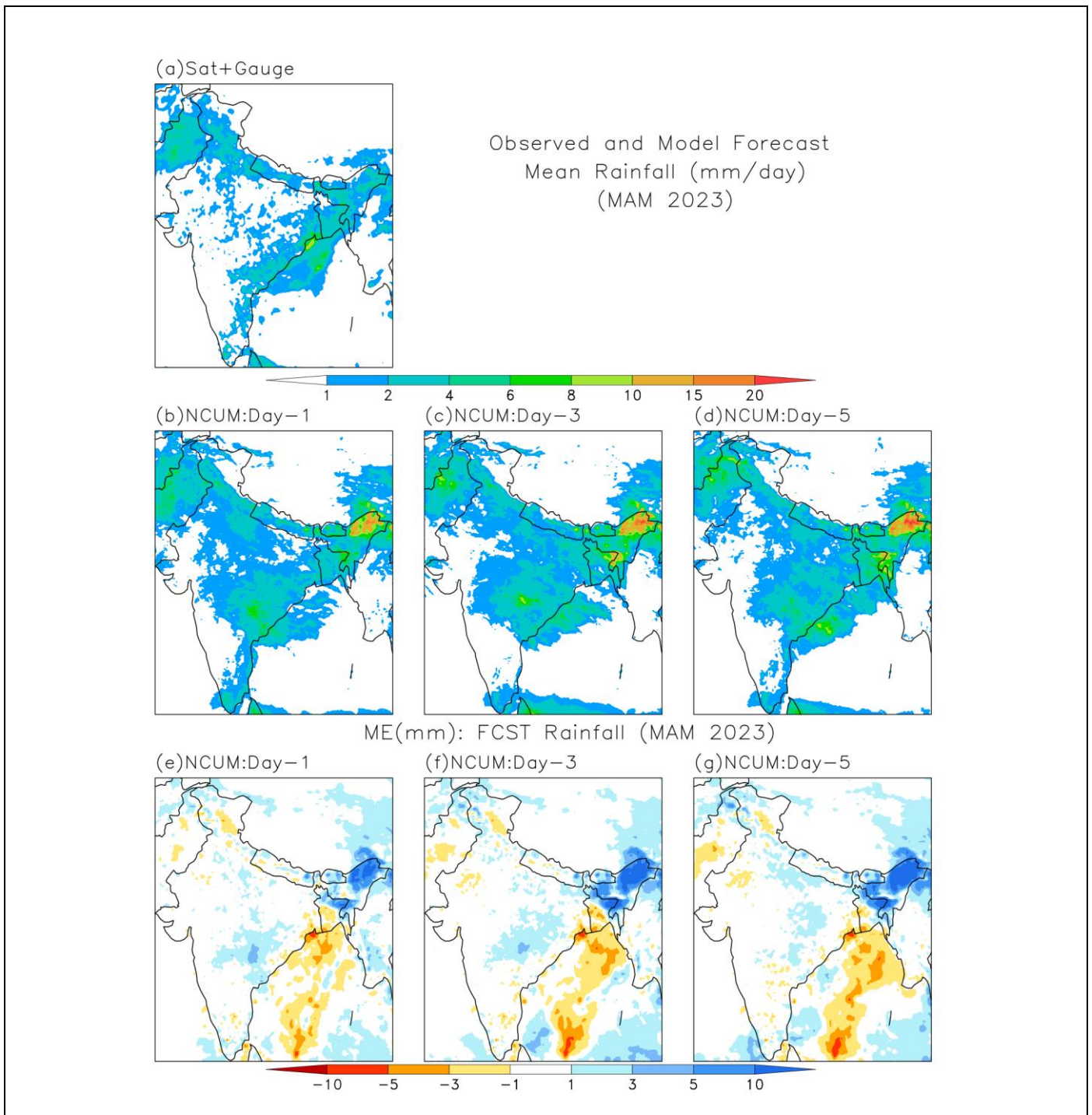


**Figure 20. Accumulated MAM rainfall (mm) in (a) Observations and (b) Day-1, (c) Day-3, and (d) Day-5 forecasts. Bottom panels (e), (f), and (g) show Mean Error (ME) in Day-1, Day-3, and Day-5 forecasts, respectively.**

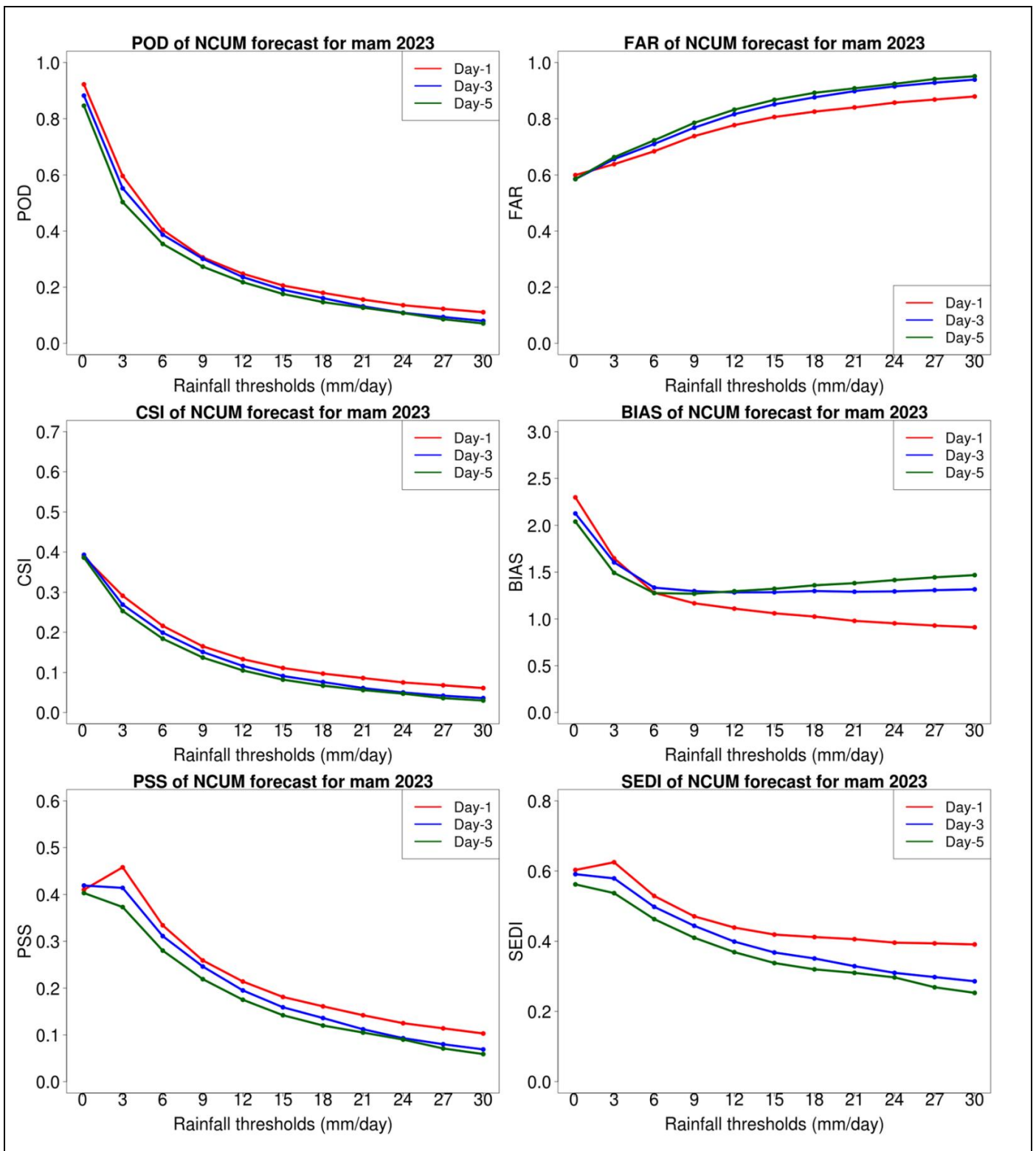
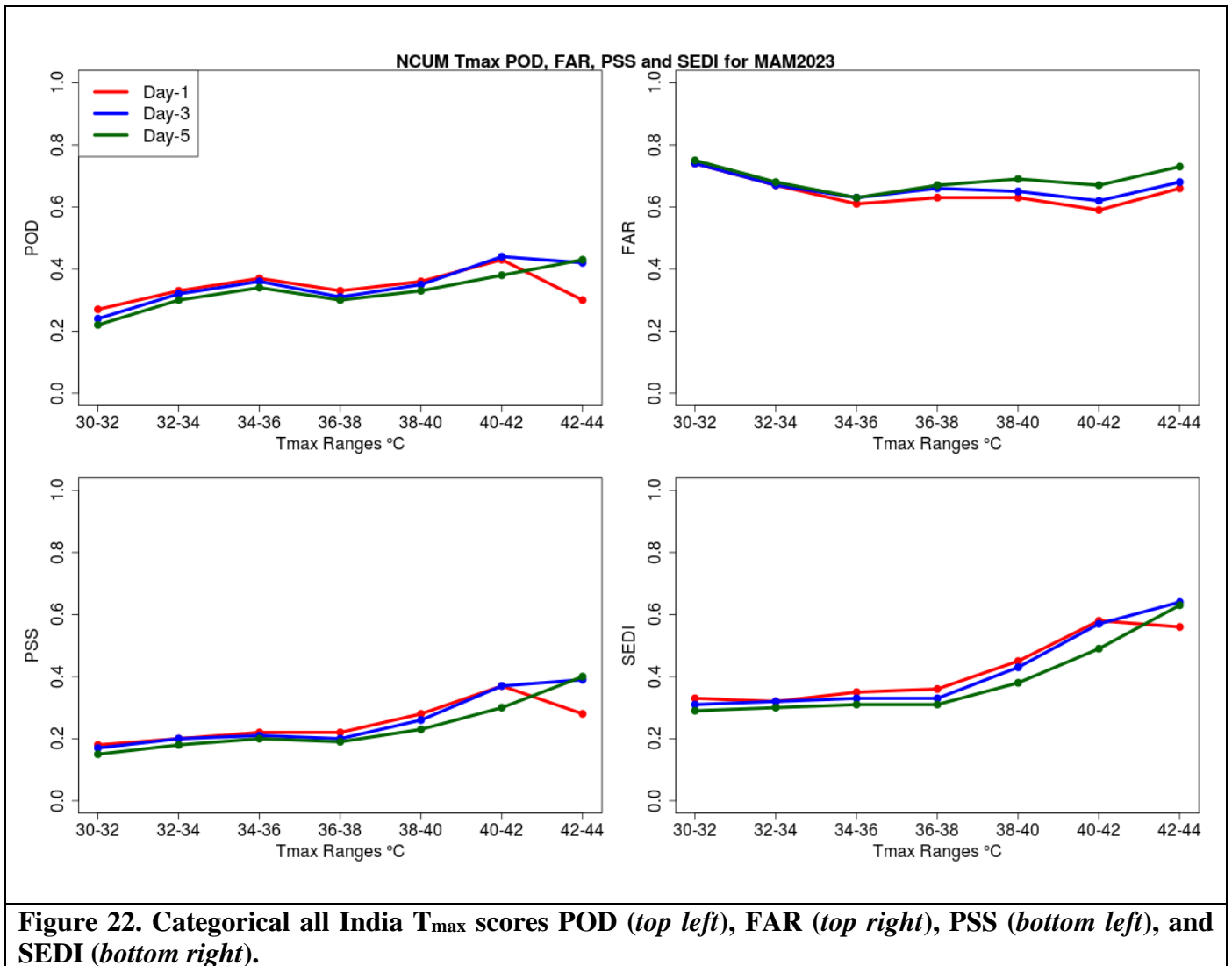


**Figure 21. Categorical all India Rainfall scores POD (top left), FAR (top right), CSI (middle left), BIAS (middle right), PSS (bottom left), and SEDI (bottom right).**



## 6. Significant Weather during MAM 2023

This section summarizes the significant weather events such as the cyclones, western disturbances, heat waves, extreme rainfall events, etc., that happened during the MAM2023 season along with the forecast assessment from the NCUM-G model.

### 6.1. Bay of Bengal ESCS ‘Mocha’ during 09-15 May 2023

This section gives a summary report on the verification of the NCMRWF model forecasts for the recent Extremely Severe Cyclonic Storm (ESCS) ‘MOCHA’ from 9-15 May 2023, which developed over the BoB. The ESCS crossed the coast between KYAUKPYU (Myanmar) and Cox’s Bazar (Bangladesh) close to North of Sittwe (Myanmar) near latitude 20.25N and longitude 92.75<sup>0</sup>E between 06-09 UTC of 14<sup>th</sup> May 2023. Verification of the forecast tracks and intensity is presented for all NCMRWF Unified Models; NCUM-G (12km grid resolution), NCMRWF Global Ensemble Prediction System (NEPS-G; 12km grid resolution),

and NCMRWF Regional Unified Model (NCUM-R; 4km grid resolution) for both 00UTC and 12UTC runs. Forecast verification is presented for model-predicted tracks and intensity against IMD best track data.

### 6.1.1. Forecast Tracks and Strike Probability

The observed and predicted tracks based on 00UTC of 12<sup>th</sup> May 2023 are shown in Figure 23 (top). All the predicted tracks indicated that ESCS Mocha would track towards Myanmar. The strike probability (Figure 23; bottom)) based on the 22-member NEPS-G ensemble indicates that the cyclone would approach the Myanmar coast in the forecast based on 12<sup>th</sup> May 2023.

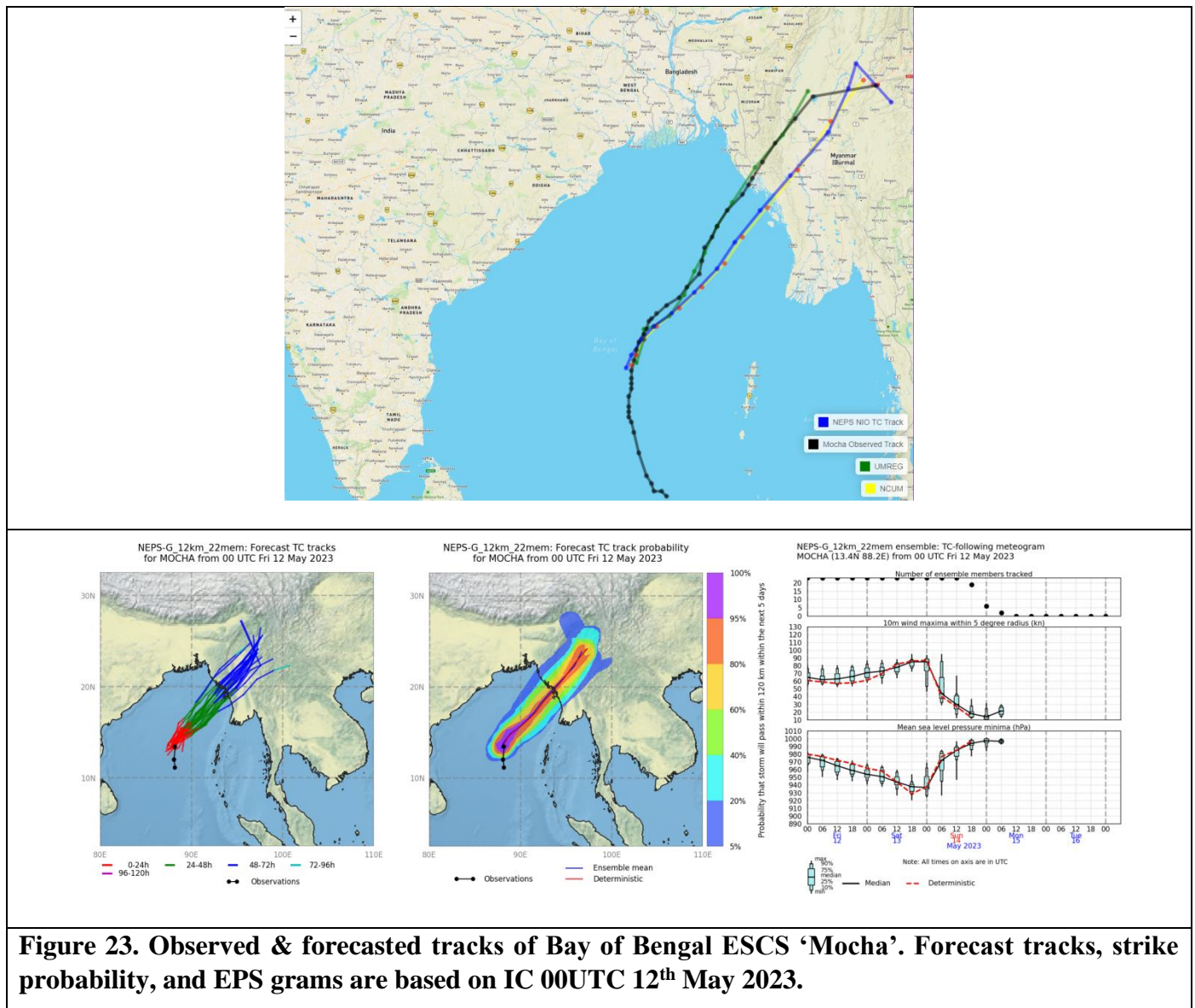


**Figure 23. Observed & forecasted tracks of Bay of Bengal ESCS ‘Mocha’. Forecast tracks, strike probability, and EPS grams are based on IC 00UTC 12<sup>th</sup> May 2023.**



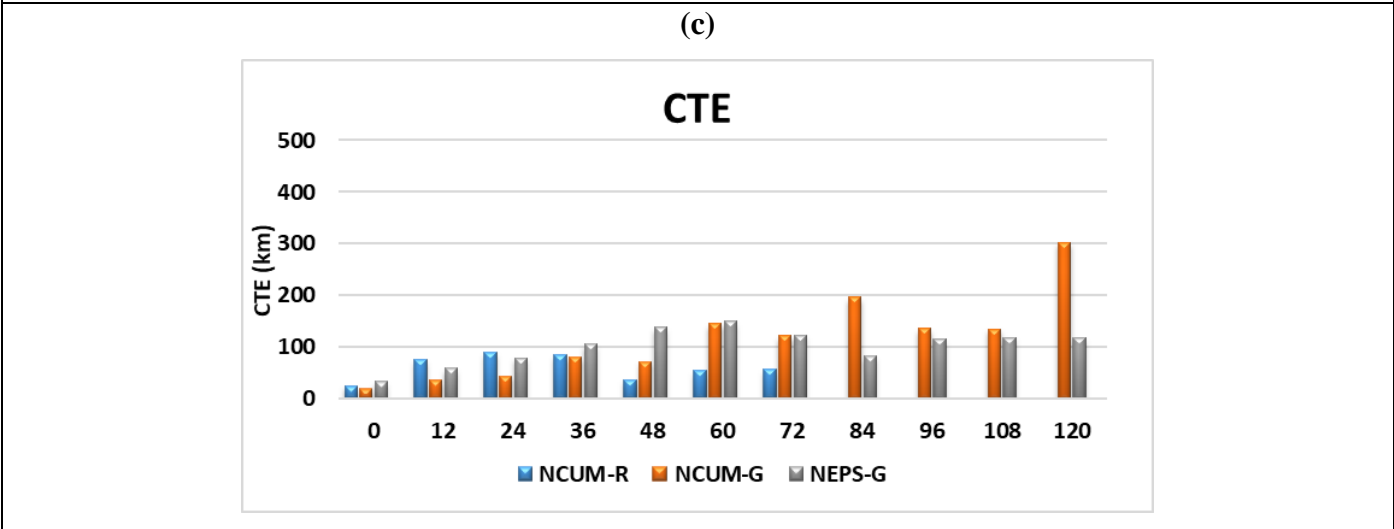
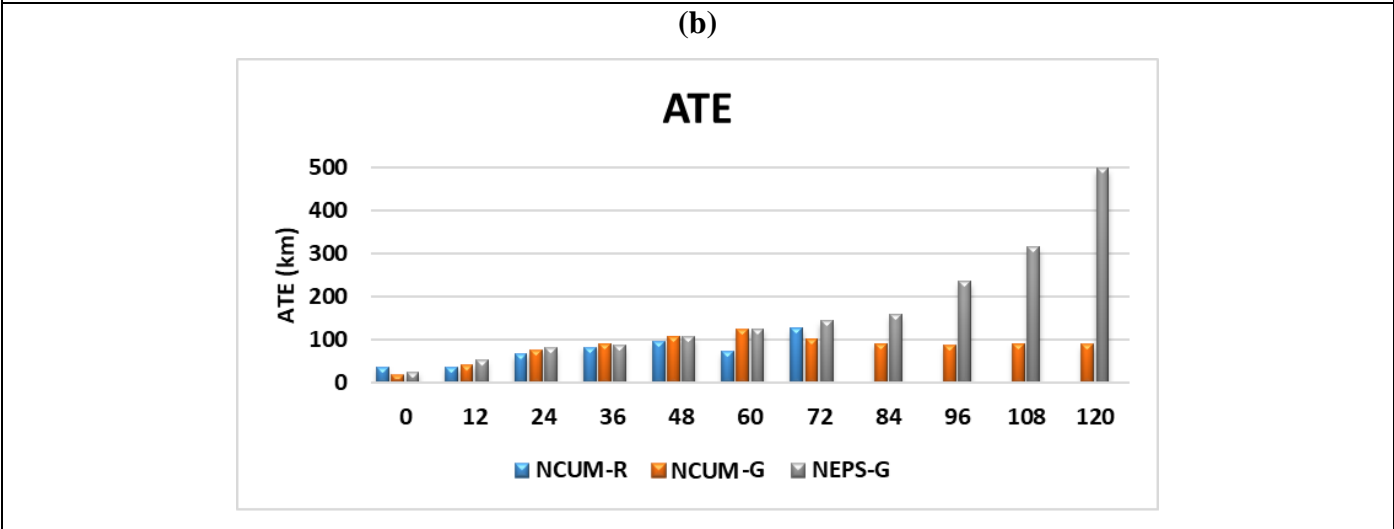
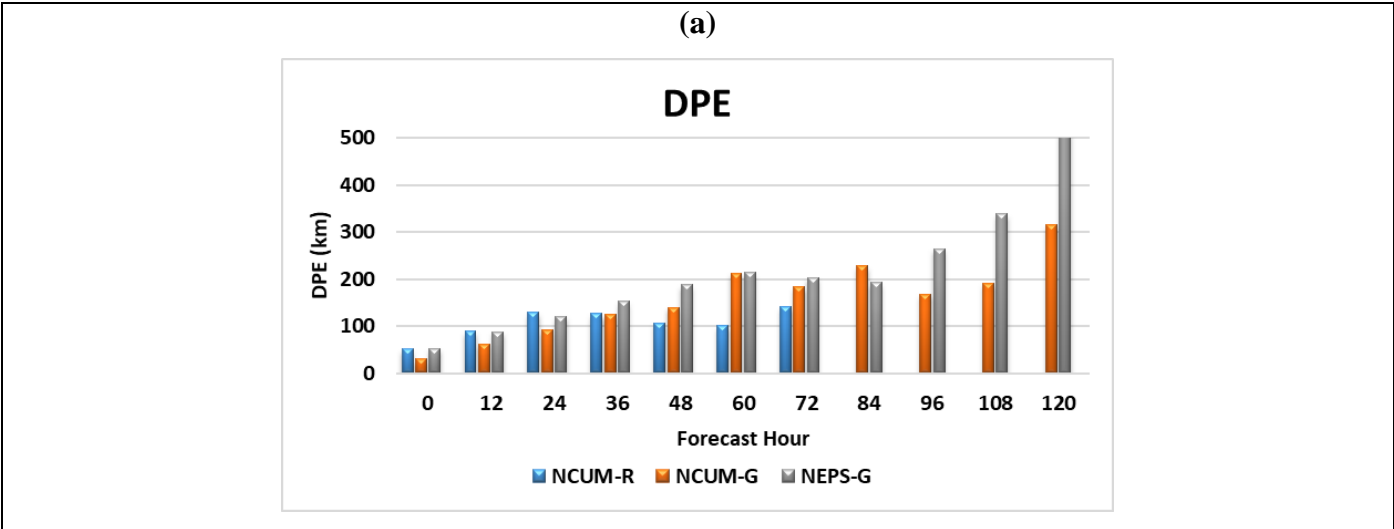
### 6.1.2. Forecast Track Errors

The NCUM-G, NCUM-R, and NEPS-G (ICs 09-14 May 2023; 00 and 12UTC runs) model forecasts have been used in the verification. Table 1 summarizes the track errors of different models. Mean initial position error is least (31 km) in NCUM-G whereas; the initial error is comparable (52 and 53 km) in both NEPS-G and NCUM-R models. NCUM-G features Direct Positional Error (DPE) <100 km up to 24 hrs.

The track error components, Direct Positional Error (DPE), Along Track Error (ATE), and Cross Track Error (CTE) are shown in Figure 24. DPE & ATE are highest in NEPS-G at all lead times. NCUM-R forecasts show higher errors till 24-hour forecasts but least after 36 hours of forecast. On the other hand, CTE is larger in NCUM-G.

**Table 1. Forecast Track Errors NCUM-R, NCUM-G, and NEPS-G (numbers in the adjacent column in italics indicate number of forecast points validated).**

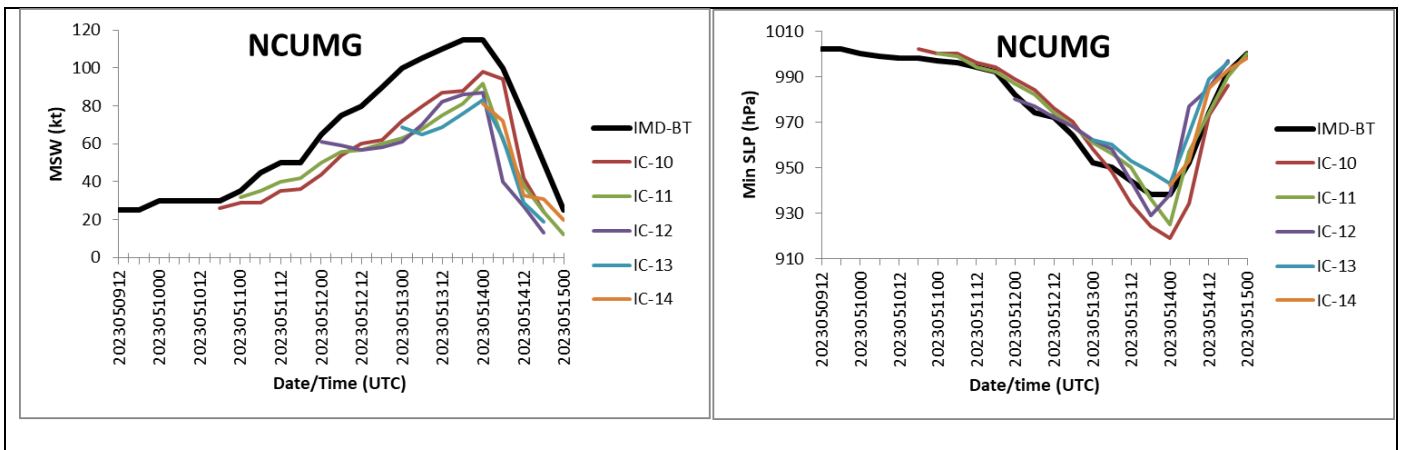
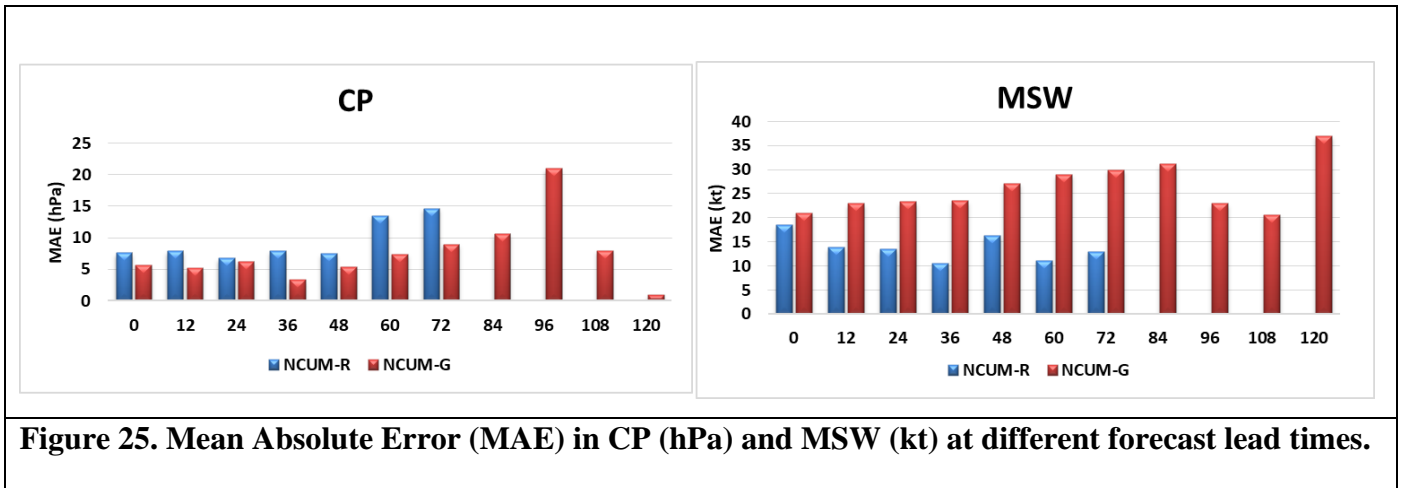
Fest Hour	DPE					
	NCUM-R	No of Fcst verified	NCUM-G	No of Fcst verified	NEPS-G	No of Fcst verified
<b>0</b>	52	9	31	9	53	<i>11</i>
<b>12</b>	89	<i>10</i>	62	9	87	<i>11</i>
<b>24</b>	129	<i>10</i>	91	9	121	<i>10</i>
<b>36</b>	126	9	124	8	152	9
<b>48</b>	107	8	139	7	188	8
<b>60</b>	101	7	213	7	214	7
<b>72</b>	141	6	183	5	203	6
<b>84</b>			228	5	192	5
<b>96</b>			168	4	264	4
<b>108</b>			192	3	338	3
<b>120</b>			315	1	512	2



**Figure 24. Track forecast errors (a) Direct Positional Error (DPE), (b) Along Track Error (ATE), and (c) Cross Track Error (CTE) in km.**

### 6.1.3. Forecast Intensity errors (Min SLP and Max Wind)

The mean absolute error (MAE) in the forecast of central pressure (CP)/minimum Sea level Pressure (min SLP) and maximum sustained wind (MSW) for NCUM-R and NCUM-G models is shown in Figure 25. The average error in MSW is low in NCUM-R. At the initial time, the MAE in CP (MSW) is <10 hPa (20 kt) in NCUM-G & NCUM-R. The magnitude of MSW is lower in NCUM-R for all lead times as compared to NCUM-G. This is also reflected in Figure 26 where both the model forecasts have very realistic representations of MSW and Min SLP with different ICs.



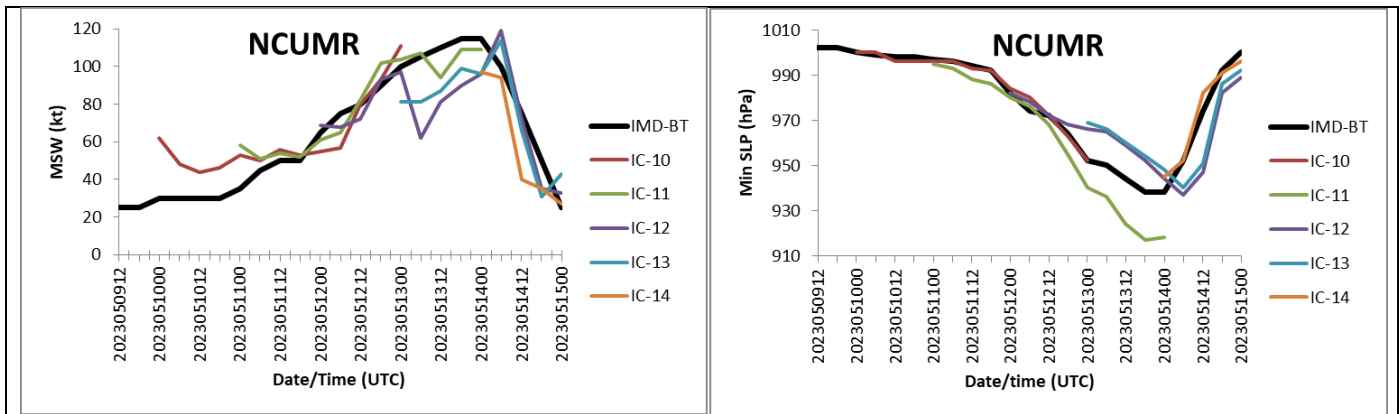


**Figure 26. Intensity given by MSW (left) & Min SLP (right) in NCUM-G (top) and NCUM-R (bottom) forecasts with different initial conditions from 9– 15 May 2023.**

### 6.1.4. Forecast Landfall Error

As per the IMD best track data, the ESCS Mocha landfall time is 06-09 UTC on 14<sup>th</sup> May and the position is 20.25<sup>0</sup>N and 92.75<sup>0</sup>E. The forecast landfall errors have been computed using the first forecast position on the land. The forecast landfall time error is -6 hours in NCUM-G from 00UTC on 11 May till 12UTC on 12 May and -3 hours from 00UTC and 12UTC on 13<sup>th</sup> May. On the other hand, NEPS-G shows a landfall time error of -6 hours from 12UTC 11 May to 00UTC 13 May. Only on 12UTC 13 May the error is -3 hours for NEPS-G forecast. NCUM-R shows the lowest landfall time error (closest to 06-09 UTC time intervals). Landfall position error was lowest in NCUM-R for 12<sup>th</sup> May 00 and 12UTC (19 km). However, NEPS-G showed the lowest errors on 13<sup>th</sup> May at 12 UTC (10 km) and 14<sup>th</sup> May at 00UTC.

**Table 2. Error in the forecasted landfall time and position (Forecasted time – Observed time) [-ve depicts early landfall and +ve shows delay in landfall]**

	NCUM-R		NCUM-G		NEPS-G	
	Position	Time	Position	Time	Position	Time
2023051100	NA	NA	281	-6	145	0
2023051112	NA	NA	100	-6	165	-6
2023051200	19	0	127	-6	100	-6
2023051212	19	0	52	-6	78	-6
2023051300	19	0	30	-3	40	-6
2023051312	35	0	45	-3	10	-3
2023051400	40	0	38	0	36	0

### 6.1.5. Verification of Strike Probability

Cyclone strike probability is the probability of locating a cyclone within 120km of any grid point. Verification of strike probability is presented using Relative Operating Characteristics (ROC) and Reliability diagrams (attributes diagrams). It must be noted that the verification of strike probability is presented for a period from 9-15 May 2023. The Reliability diagram gives a comparison of forecast probability against the observed frequencies. A perfect match will show all points along the diagonal line. Points above the diagonal suggest underestimation (lower forecast probabilities) while points below the diagonal suggest overestimation (higher forecast probabilities).

For the case of ESCS “Mocha”, the verification of strike probability obtained from NEPS-G is carried out using the best track data. Figure 27 shows the reliability and ROC plots for the strike probability verification. In the Reliability diagram, the points along the diagonal indicate the best-performing model. While some points below the diagonal indicate over-estimation of cyclone strike probability. The ROC curve of NEPS-G shows that the model has skill as the curve is away from the diagonal line of no resolution. The AROC (area under the ROC) is 0.7 which is also indicative of reasonably good resolution in the model.

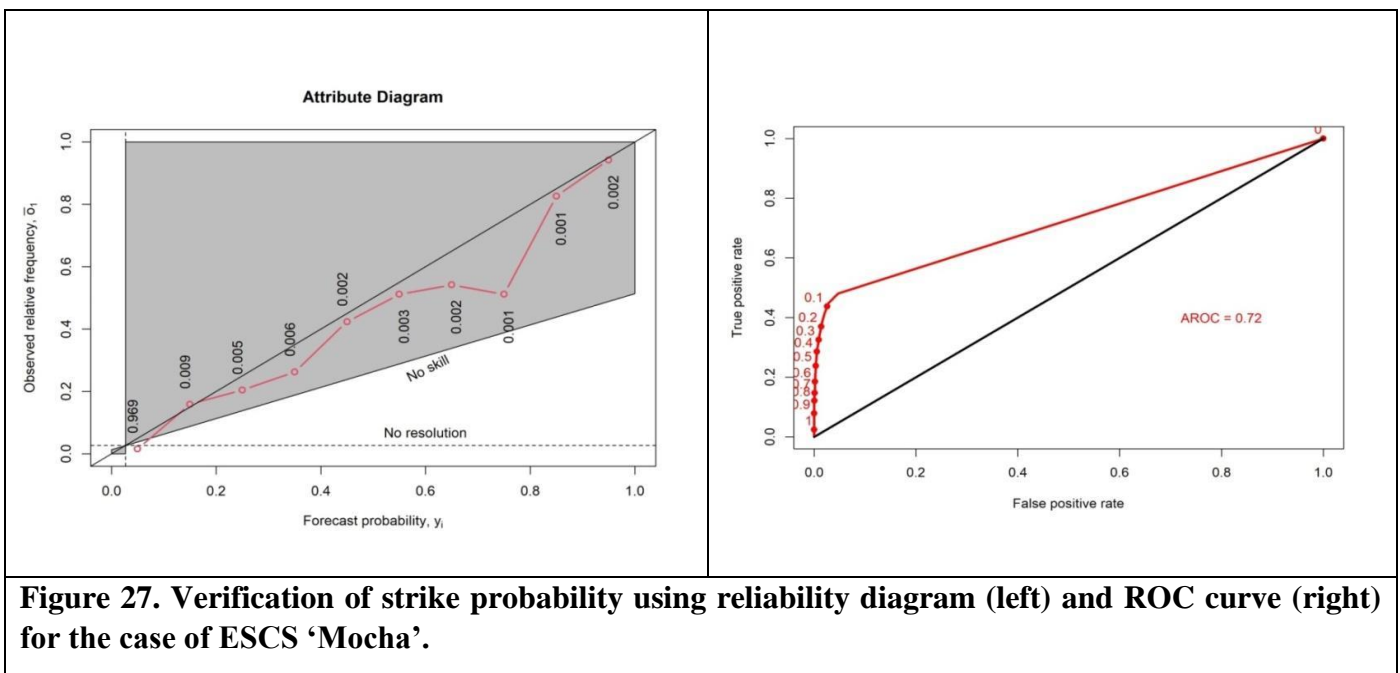


**Figure 27. Verification of strike probability using reliability diagram (left) and ROC curve (right) for the case of ESCS ‘Mocha’.**

### 6.1.6. CRA Verification of Rainfall Forecasts

Contiguous rain areas (CRA) verification is a spatial verification method (Ebert and Gallus 2009) that focuses on individual weather systems and verifies the properties of the forecast objects, which allows the estimation

of location error of the forecast entity. A detailed description of the method with the application over India can be found for UM Rainfall forecasts over India (Ashrit et al 2015a) and MoES Models (NCUM & GFS) in Sharma et al., (2020). Here, NCUM-G rainfall forecasts corresponding to the ESCS ‘Mocha’ on 14<sup>th</sup> and 15<sup>th</sup> May 2023 are discussed briefly using CRA verification (Figure 28a-d). The results are presented for Day-3 (*left panels*) and Day-5 (*right panels*) forecasts valid on 14<sup>th</sup> May 2023 (*top*) and 15<sup>th</sup> May 2023 (*bottom*). The CRA verification is presented for 40 mm/day threshold.

On 14<sup>th</sup> May 2023, prior to the landfall, the cyclone is near the coast, and observed rainfall is mainly confined to the Sea and away from the Myanmar coast. The Day-3 forecasts overestimate all attributes ‘*grid points > 40mm*’ (i.e., spatial coverage), ‘*Average Rainfall*’, ‘*Maximum Rain*’, and ‘*Rain volume*’. On the other hand, the Day-5 forecasts underestimate all attributes. The Day-3 and Day-5 forecasts completely miss the observed rainfall over the northwest part of coastal Myanmar. In the Day-3 forecast, the 40mm/day object is shifted by 1.48° southwards and 1.46° eastwards. In the Day-5 forecast, the object is shifted by 0.20° westwards and 1.45° southwards. Contribution to RMSE from pattern error is dominating (51.1% in Day-3 and 71.1% in Day-5 forecasts) and next by displacement (42.3% in Day-3 and 28.1% in Day-5 forecasts).

Similarly, on 15<sup>th</sup> May 2023 (Figure 28 c, d), the observed rainfall (*top left panels*) the rainfall covers partly over Sea and partly over Myanmar. The forecasts overestimate all the attributes in Day-3 and Day-5. In the Day-3 forecast, the 40mm/day object is shifted by 1.45° eastwards and 0.35° northwards. In the Day-5 forecast, the object is shifted by 1.46° eastwards and 0.45° northwards. In this case, the contribution to RMSE is mainly from the pattern error (64.7% in Day-3 and 51.2% in Day-5) followed by volume error (26% in Day-3 and 42% in Day-5).

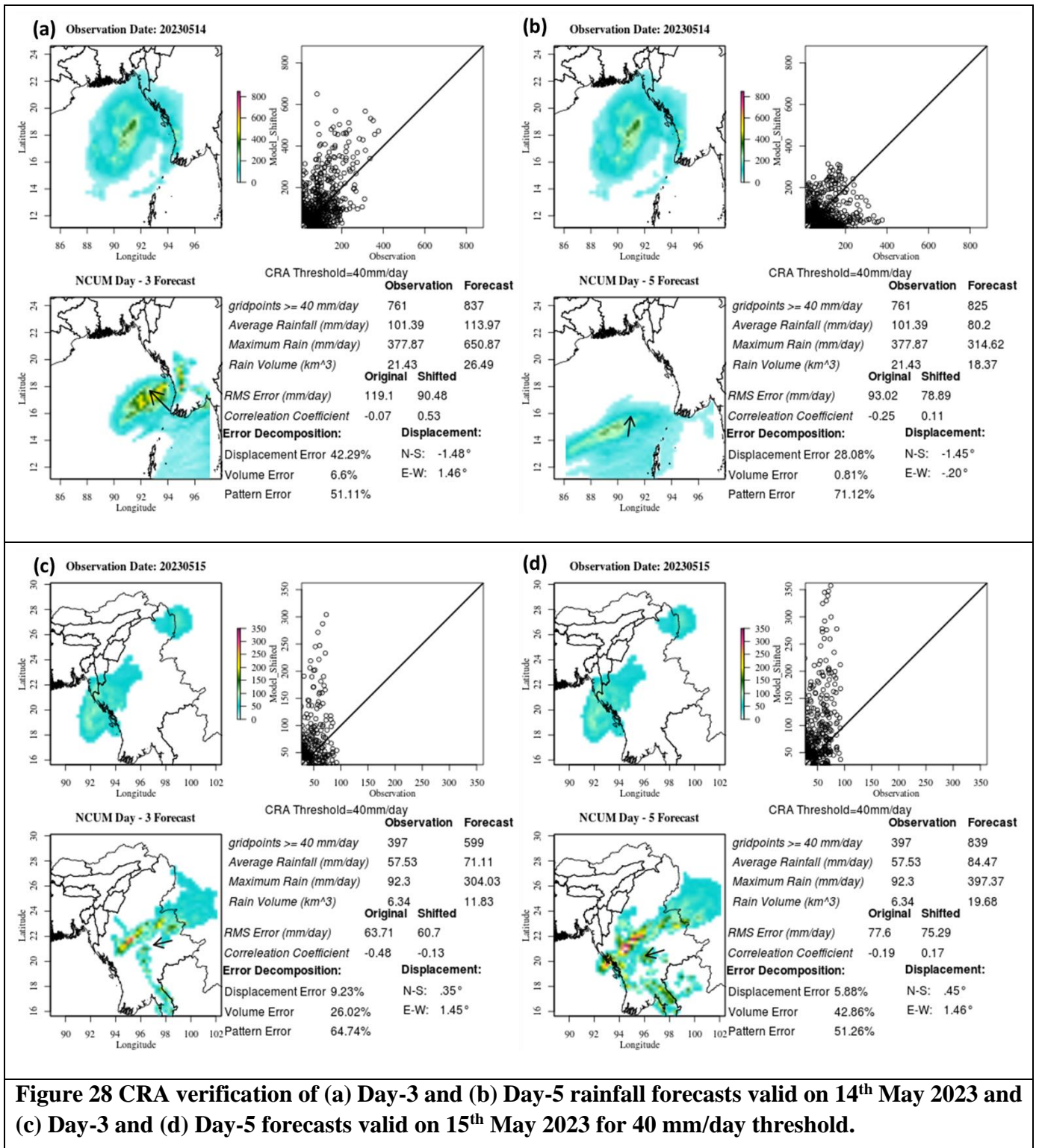


**Figure 28 CRA verification of (a) Day-3 and (b) Day-5 rainfall forecasts valid on 14<sup>th</sup> May 2023 and (c) Day-3 and (d) Day-5 forecasts valid on 15<sup>th</sup> May 2023 for 40 mm/day threshold.**

## 6.2. Western Disturbance & Heat waves

### 6.2.1. Western Disturbance

A WD is usually driven by the westerlies that originate in the Mediterranean region and brings rainfall to the northwestern parts of the country. Out of all the WDs as per IMD during the pre-monsoon season (MAM), 2023 listed in Table 3, we have chosen a WD case for this report. Here we verify a WD that occurred during 29-31 May 2023. The trough in middle tropospheric westerlies can be seen in Figure 29 (top left panel) on 29<sup>th</sup> May 2023, with its axis running roughly along the longitudes 72-75<sup>o</sup>E. The NCUM-G forecasts clearly predicted this trough in Day-1 to Day-5 forecasts. The associated rainfall is primarily over the Northwest India and central India (Figure 30a). The NCUM-G model predicted the rainfalls associated with this trough in Day-1 to Day-3 forecasts with magnitudes closer to the observations with less rainfall amounts in Day-4 and Day-5 (Figure 30).

**Table 3. List of MAM seasonal Western Disturbances.**

S. No.	Month	Western Disturbances (WDs)	
		Total	Duration
1.	March	7	1- 3 Mar, 5-11 Mar, 13-16 Mar, 15-20 Mar, 19-22 Mar, 22-28 Mar, and 28-31Mar.
2.	April	5	2-6 Apr, 14-19 Apr, 21-25 Apr, 25-29 Apr, and 28-30 Apr.
3.	May	8	1 – 4 May, 4 – 11 May, 11 – 16 May, 15 – 17 May, 17- 22 May, 23 – 28 May, 27 – 28 May, and 29-31 May.



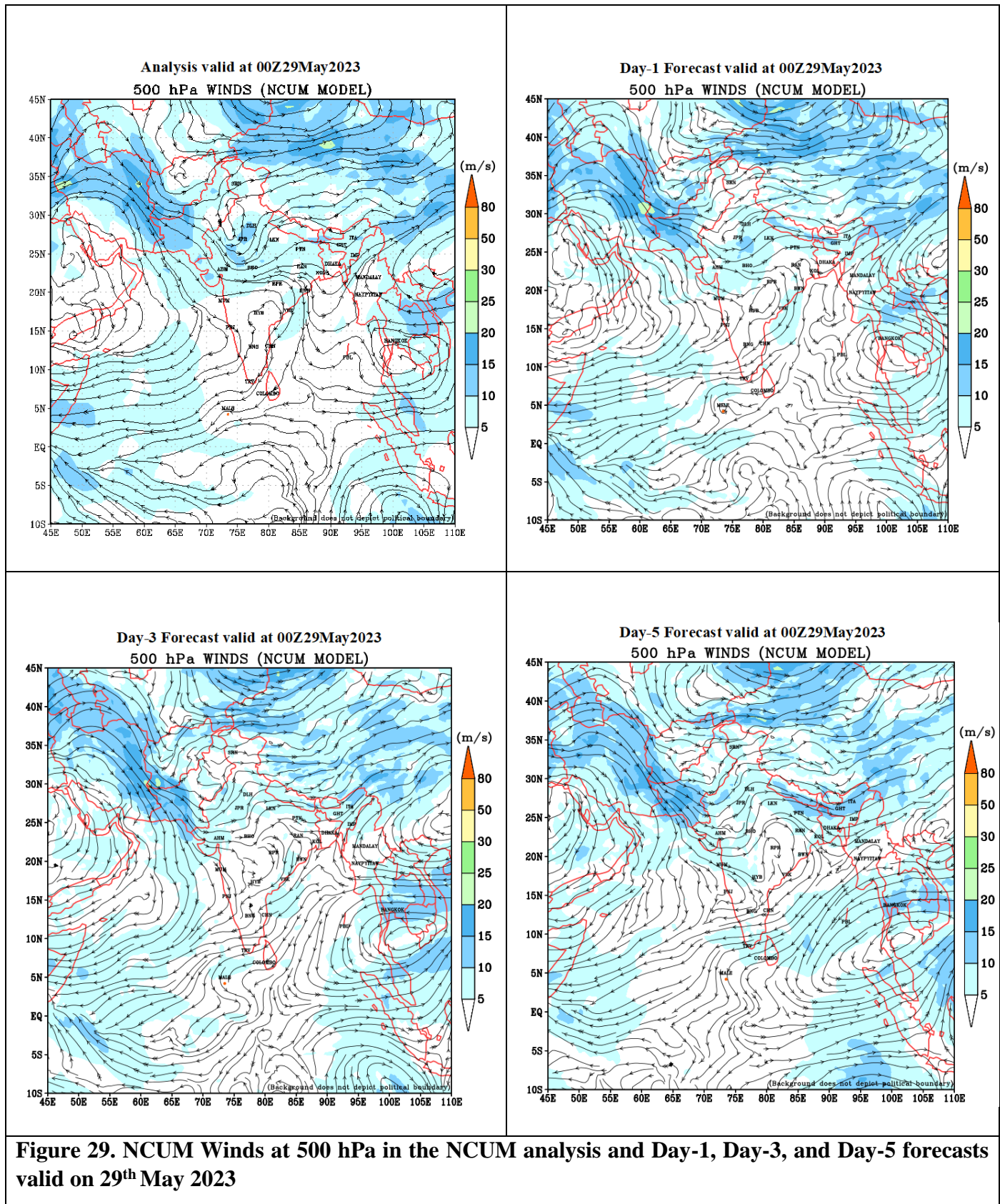


**Figure 29. NCUM Winds at 500 hPa in the NCUM analysis and Day-1, Day-3, and Day-5 forecasts valid on 29<sup>th</sup> May 2023**

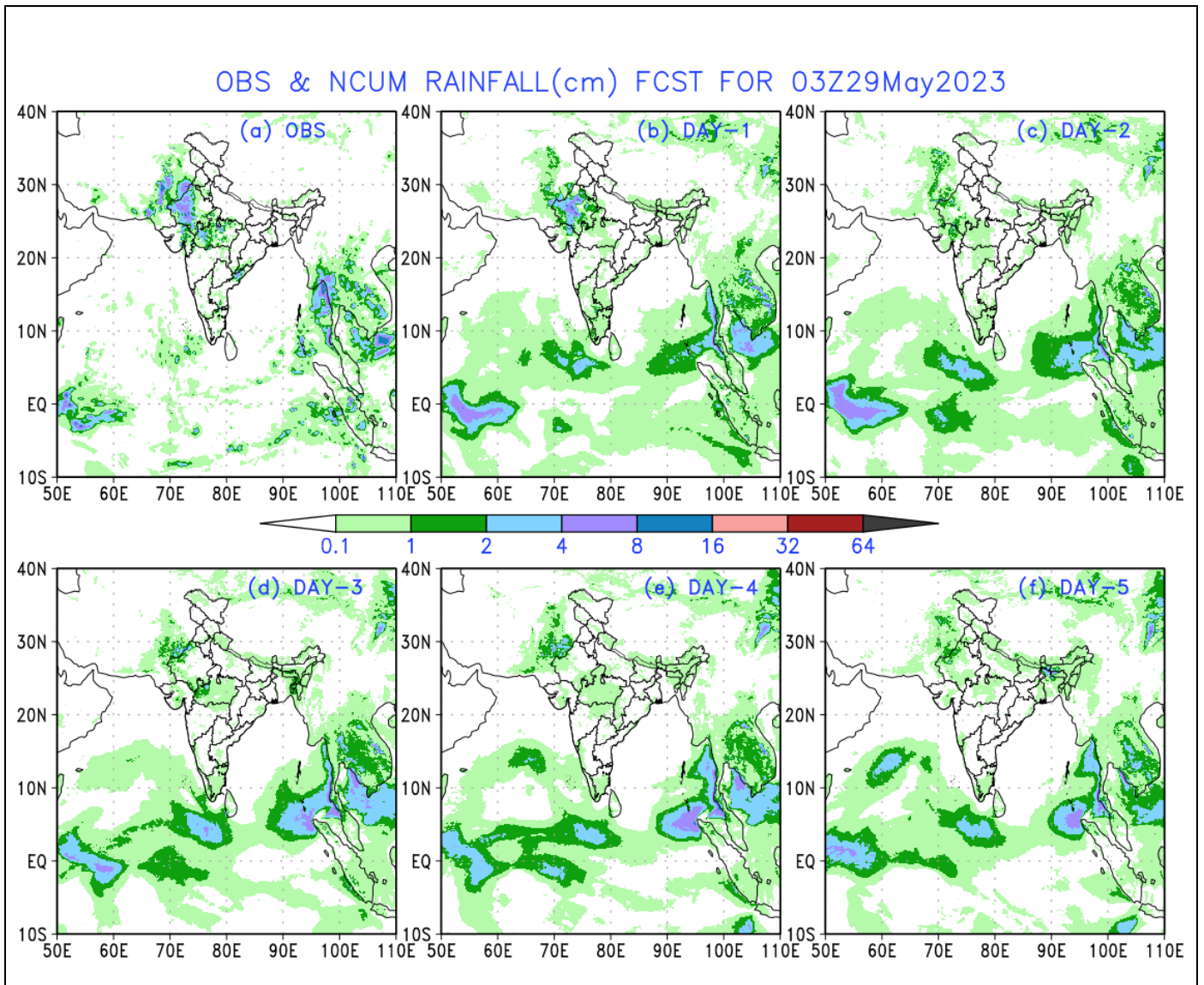


**Figure 30. Rainfall (cm/day) from (a) IMD-observations (b) Day-1, (c) Day-2, (d) Day-3, (e) Day-4, and (f) Day-5 forecasts of NCUM on 29<sup>th</sup> May 2023.**

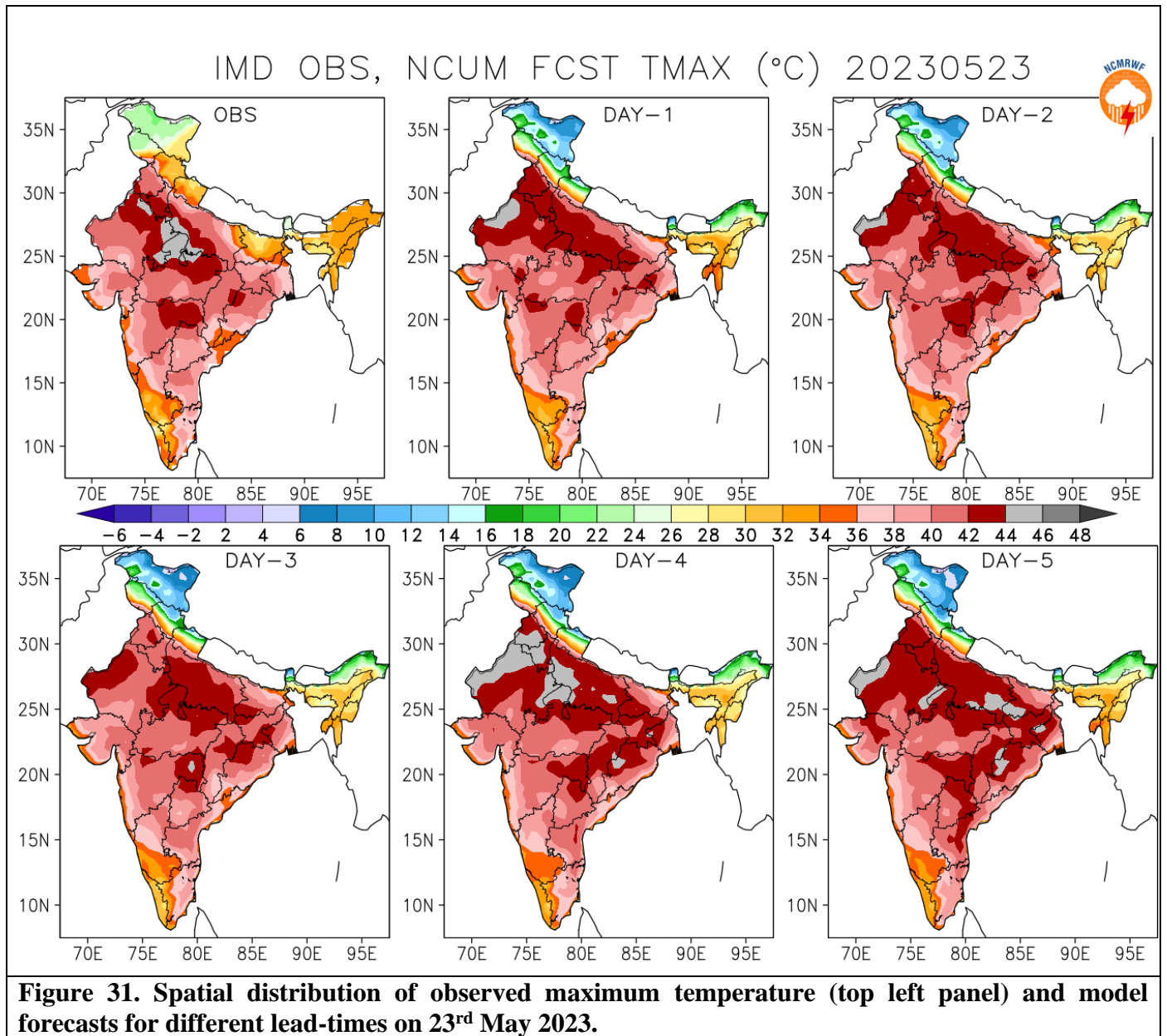
### 6.2.2. Heat Waves

India has experienced multiple heat wave events during MAM 2023. As per the IMD report, specifically April 2023, was the warmest. During this month the average maximum temperature ( $T_{max}$ ) was above normal by  $4.5^{\circ}\text{C}$  over most parts of East & Northeast India and coastal parts of South Peninsular India. Heat wave events as reported by IMD during the pre-monsoon season (MAM), 2023 are listed in Table 4. Here, we verify the heat wave event that occurred over Delhi, South Uttar Pradesh, West Rajasthan, and Northeast Madhya Pradesh from 22-24<sup>th</sup> May 2023. Figure 31 shows the temperature distribution on the middle of the heatwave event on 23<sup>rd</sup> May 2023 with the highest temperatures of more than  $40^{\circ}\text{C}$  is recorded over the northern western and central parts of India. The spatial distribution of  $T_{max}$  is well predicted in the NCUM-G model forecasts

till Day-5. Moreover, models have well captured the spatial distribution of maximum temperature above 42°C along the IGP. However, temperature above 44°C is underestimated in Day-1 to Day-5 forecasts.

**Table 4. List of MAM seasonal Heat Wave Events**

<b>S.No.</b>	<b>Month</b>	<b>Heat Wave Events</b>
<b>1.</b>	March	No heat wave event
<b>2.</b>	April	<ul style="list-style-type: none"> <li>❖ West Bengal, Bihar, Odisha, and Coastal Andhra Pradesh during <b>12-20 April</b> and they <b>lasted for</b> 9, 7, 5, and 4 days, respectively, during this period.</li> <li>❖ For <b>northwest India and west-central India</b>, it was highly <b>sub-dude</b> (i.e., only for 1-3 days over Punjab, Haryana, Chandigarh, Delhi, and Uttar Pradesh).</li> <li>❖ Konkan &amp; Goa and Jharkhand also experienced 1 day of Heat Wave activity in April 2023.</li> <li>❖ Northeast India also reported higher than normal day temperatures on most dates during 11-22 April 2023.</li> </ul>
<b>3.</b>	May	<ul style="list-style-type: none"> <li>❖ West Bengal &amp; Sikkim and Bihar during <b>9-11 May</b></li> <li>❖ Gujarat during <b>11-12 May</b></li> <li>❖ West Rajasthan during <b>12-13 May</b></li> <li>❖ Coastal Andhra Pradesh during <b>15-17 May</b></li> <li>❖ Delhi on <b>22 and 23 May</b></li> <li>❖ South Uttar Pradesh from <b>21-23 May</b></li> <li>❖ West Rajasthan on <b>21 and 22 May</b></li> <li>❖ Northeast Madhya Pradesh during <b>22-24 May</b></li> </ul>



### 6.2.3. Observed and forecasted daily Tmax time series

Further, verification of the Tmax forecasts based on the NEPS ensemble is shown for several locations over Northwestern India. Observed Tmax data is obtained from SYNOP stations over India via the GTS network. Figure 32 shows the forecasts with IC of 17<sup>th</sup> May 2023 for Amritsar, 18<sup>th</sup> May 2023 for Jaipur and Jodhpur, and 19<sup>th</sup> May 2023 for Delhi. The NEPS control (red), ensemble mean (blue), and ensemble members (green) are compared with the observations (black). Observed Tmax generally lies within the spread of ensemble members. Ensemble mean shows a very good match with the observations and successfully predicts a sharp rise/fall in value consistent with observations. The sharp increase in observed Tmax in Amritsar by about

~6<sup>0</sup>C between 19 -24<sup>th</sup> May 2023 is accurately predicted. Similarly, for IC of 18<sup>th</sup> (19<sup>th</sup> May 2023), the heatwave event over Jaipur and Jodhpur (Delhi) during 21-23<sup>rd</sup> (22-23<sup>rd</sup>) May 2023 is also well captured.

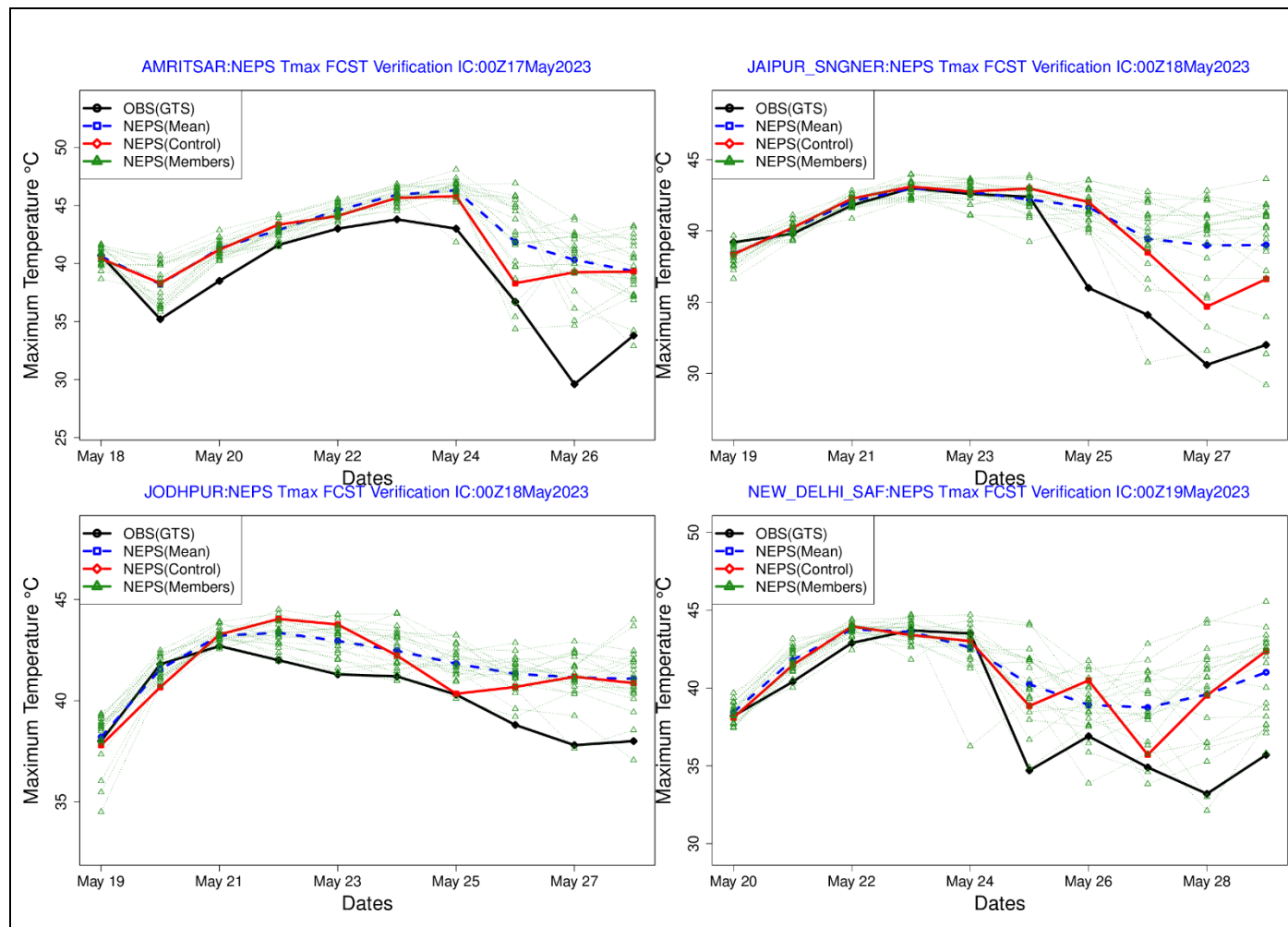


**Figure 32. Observed and NEPS-G forecast Tmax over different cities over North India during the heat wave conditions of May 2023.**

## 7. Summary

This report documents the performance of the NCMRWF model forecasts during the Pre-monsoon season MAM 2023. The verification results are presented to address both forecasters and model developers. The information on biases in the forecast winds, temperature, humidity, rainfall, etc., is crucial for the forecasters to interpret the model guidance for forecasting. Additionally, information on recent improvements in the model skill adds to confidence in the model forecasts. The results of the study can be summarized below.

## 7.1. NCUM-G Mean analysis and anomalies during MAM 2023

- ❖ *The low-level winds at 850 hPa and 700hPa represent northwesterly winds with increasing altitudes having strength ranging from 5 to 10 m/s and the presence of anticyclone over the southern peninsular region. Further, with increasing altitude, mean winds in the north Indian region enhanced from ~18m/s at 500 hPa to more than 40m/s in the upper troposphere.*
- ❖ *The anomalous winds at 850hPa and 700hPa indicate contrasting features in the north and south with weaker and stronger winds in NCUM-G analysis with respect to ERA5 reanalysis, respectively, over the Indian subcontinent. At 850 hPa level, an anomalous cyclonic circulation is present over northwestern India. This circulation is becoming enhanced at 700 hPa level w.r.t ERA5. On the other hand, over the equatorial Indian Ocean, specifically in southern latitudes, the winds are weaker in NCUM-G analysis resulting in strong anomalous easterlies. Overall, in north India, the magnitude of winds is relatively lower compared to ERA5 reanalysis due to persistent anomalous easterlies.*
- ❖ *Low level (850 and 700 hPa) temperature anomalies indicate the Pre-monsoon 2023 is cooler than the climatology with magnitudes between more than  $-1^{\circ} \sim -2^{\circ}\text{C}$  in the northwest and central parts of India. The cooler temperatures stretch from northwest to southeast India covering the Indo-Gangetic plains. The temperature anomalies across India still indicate cooler (warmer) than the climatology at 500 (200) hPa level.*
- ❖ *MAM 2023 indicates a higher percentage of RH compared to the climatology across India. The Oceanic regions of the Bay of Bengal and Arabian seas also showed positive anomalies in the humidity distribution for the Pre-monsoon period and negative anomalies are noted in the equatorial regions at lower levels (i.e., at 850 and 700 hPa).*

## 7.2. NCUM-G Systematic Errors

- ❖ *Systematic errors in winds at 850 hPa from Day-1 forecasts show a westerly wind bias over the northern Indian region and along the west coast. Enhanced north westerlies are more prominent along the west coast. With forecast lead times these errors in low-level winds enhance and this could be due to the enhanced convective activity around the equatorial regions during the Pre-monsoon season. Similar systematic errors in winds are also noticed at 700 hPa level over the Indian region. In addition, westerly wind bias is more prominent at 700 hPa level over the eastern equatorial Indian Ocean in Day-3 and Day-5 forecasts. Systematic errors at 200 hPa level winds show enhanced divergent circulation centered around central parts of India as seen in Day-3 forecasts and a similar spatial pattern in winds is also seen in Day-5 forecasts with enhanced error magnitudes.*
- ❖ *The model shows warm bias ( $\sim 1\text{-}3^{\circ}\text{C}$ ) occupied over most of the Indian land mass and the magnitude of this bias is increasing with forecasts lead time. These error increments at 850 hPa temperatures are also more prominent over IGP regions. On a similar note, temperature errors at 700 hPa also show warm bias ( $>1^{\circ}\text{C}$ ) over most of the Indian land region. Interesting to see that the bias over the south AS region reverse sign and now exhibits warm bias compared to the 850 hPa level. At 500 hPa (200 hPa) level, temperature exhibits warm (cold) bias over the Indian land region including surrounding oceanic regions, and the magnitude of the bias is increasing in forecasts with lead time.*

- ❖ *Systematic errors show a large dry bias over Indian land regions at 850 hPa level, and this dryness is enhancing with forecasts lead time. The presence of low-level anticyclones over the Indian subcontinent induces enhanced warming, which could be one primary reason for the negative RH values over the central Indian region. On the contrary, oceanic regions exhibit moist bias as evidenced by positive RH values, except for Africa and West Arabian regions. Interestingly the moist bias observed over the oceanic regions (i.e., AS and BoB) at 850 hPa level change sign to negative, and dry bias is seen at 700 hPa level. Additionally, the moist bias south of the equator is getting intensified in the Day-3 and Day-5 forecast and the entire column is occupied with excess moisture at 700 hPa levels*
- ❖ *Seasonal mean winds at 10m level from the analysis show the presence of relatively strong north westerlies over the Arabian Sea (AS), south-westerlies over head BoB, and weak westerlies over the tropical Indian Ocean (TIO) while below TIO strong easterlies around 80°E. The systematic error in the forecasts depicts few notable features --(i) The north-westerly wind bias along the west coast over northern AS and south-westerly wind bias along the east coast over BoB on Day-1 forecast is enhancing its strength with forecasts lead time. (ii) On a similar note, the easterly wind bias seen in the Day-1 forecast around the equator and south of the equator close to the maritime continent is also getting intensified in the Day-5 forecast.*
- ❖ *Systematic errors show a relatively warm bias over the Indian land regions. Interestingly this warm bias is increasing with forecast lead time. This can be attributed to the dry northwesterly winds from the northwest entering Indian land and north AS. In addition, most of the oceanic regions of BoB and AS exhibited cold bias in the range  $< -0.5^{\circ}\text{C}$  in all the forecast times.*
- ❖ *Seasonal mean PWAT shows a large value ( $> 60\text{mm}$ ) around the equatorial regions, especially over the Maritime continent (MC) owing to the presence of warm pools and associated convection during pre-monsoon season over these regions. On the contrary, most of the northern and central Indian regions are dry with very less PWAT values (5-25mm). However, extreme Southeast peninsular India exhibits moderate PWAT values around 35-40 mm due to the westerly winds from the MC region. Systematic error in PWAT shows a column dry over Indian land regions on Day-1, this dryness in the column is enhancing with forecast lead time, and its magnitude is maximum on Day-5.*

### **7.3. Forecast Verification**

- ❖ *Much of the Indian subcontinent is dry except for the northern parts of India, the southern parts of peninsula India, regions along the eastern coast, and the northeastern regions. NCUM-G model forecasts overestimate the rainfall particularly over the central India, along the eastern coast and the northeastern regions while underestimating over the oceanic regions.*
- ❖ *For different rainfall thresholds (3-30mm/day) POD (FAR) shows a decrease (increase) in scores.  $\text{POD} \geq 0.3$  for rainfall up to 6 mm/day. The BIAS score (frequency bias) indicates that forecasts overestimate the frequency of all thresholds. The values of PSS and SEDI up to 3-5 mm/day indicate reasonable skill.*
- ❖ *The categorical scores for Tmax are also computed for MAM 2023. The POD indicates a slight increase with the thresholds from 30°C to 44°C while the PSS score is nearly constant and below 0.3 till 40°C, thereafter it slightly increases to above 0.3. FAR scores overall India as a whole*

show relatively large values  $>0.6$  up in all temperature thresholds and varies between 0.6-0.8 in all forecast lead times.

#### 7.4. Verification for Significant Weather

Bay of Bengal ESCS 'MOCHA' during 9-15 May 2023, Western Disturbances, and Heat waves formed significant weather events of MAM 2023.

- ❖ **Initial Position Error:** Mean initial position errors are lower in NCUM-G (31 km).
- ❖ **Direct Position Error:** NCUM-G shows track errors less than 100 km up to 24 hrs. NCUM-R shows the lowest track error from the 24 to 72-hour forecast. DPE in mean NEPS-G is the highest at all lead times.
- ❖ **Landfall Position & Time error:** The landfall position errors  $<20$  km are seen from NCUM-R on 12<sup>th</sup> May forecasts (00UTC and 12UTC) and 13<sup>th</sup> May (00UTC) and in NEPS-G with the lowest error ( $<\sim 10$ km) on 13<sup>th</sup> May (12UTC) and 14<sup>th</sup> May (00UTC). Landfall time errors in both global models are  $\sim -6$  h (faster) from 11<sup>th</sup> to 13<sup>th</sup> May. The best forecast in terms of landfall time is seen in NCUM-R for both 00 and 12 UTC in all forecast days.
- ❖ **Intensity verification (NCUM-G & NCUM-R):** MAE in MSW is lower in NCUM-R.
- ❖ **Verification of strike probability (NEPS-G & NEPS-R):** ROC and Reliability diagrams are used for this purpose. The NEPS-G model is over-forecasting. The ROC curves show that the models have reasonable skill (ROC is 0.72).
- ❖ We have also verified a WD that occurred during 29-31 May 2023. The trough in middle tropospheric westerlies can be seen on 29<sup>th</sup> May 2023, with its axis running roughly along the longitudes 72-75<sup>0</sup>E. The NCUM-G forecasts predicted this trough on Day-1 to until Day-5 forecasts. This western disturbance brought rainfall primarily over Northwest and central India. The NCUM-G model predicted the rainfalls associated with this trough in Day-1 to Day-3 forecasts with magnitudes closer to the observations with lower rainfall amounts on Day-4 and Day-5.
- ❖ Further, during MAM 2023 heatwave conditions are verified from model forecasts against observations for different forecast lead times. Overall, the heat wave conditions are predicted very well 3 days earlier, and after that model skill is reduced.



## References

1. Ashrit, R., Elizabeth Ebert, Ashis K. Mitra, Kuldeep Sharma, Gopal Iyengar and E.N. Rajagopal 2015a: Verification of Met Office Unified Model (UM) quantitative precipitation forecasts during the Indian Monsoon using the Contiguous Rain Area (CRA) method. NMRF/RR/03/2015
2. Ashrit R, Sharma K, Dube A, Iyengar G R, Mitra A K and Rajagopal E N 2015b: Verification of short-range forecasts of extreme rainfall during monsoon; *Mausam* 66 375–386, 607.
3. Barker, D., 2011. Data assimilation-progress and plans, MOSAC-16, 9-11 November 2011, Paper16.6.
4. Ebert, E.E. and W.A. Gallus, 2009: Toward better understanding of the contiguous rain area (CRA) method for spatial forecast verification. *Wea. Forecasting*, 24, 1401-1415.
5. Hersbach H, Bell B, Berrisford P, et al. 2020: The ERA5 global reanalysis. *Q J R Meteorol Soc.* 2020;146:1999–2049. <https://doi.org/10.1002/qj.3803>
6. Jolliffe, I. T., and D. Stephenson, 2012: *Forecast Verification: A Practitioner's Guide in Atmospheric Science*, John Wiley & Sons, Ltd.
7. Kumar Sumit, A. Jayakumar, M. T. Bushair, Buddhi Prakash J., Gibies George, Abhishek Lodh, S. Indira Rani, Saji Mohandas, John P. George and E. N. Rajagopal 2018: Implementation of New High Resolution NCUM Analysis-Forecast System in Mihir HPCS. NMRF/TR/01/2019, 17p.
8. Kumar Sumit, M. T. Bushair, Buddhi Prakash J., Abhishek Lodh, Priti Sharma, Gibies George, S. Indira Rani, John P. George, A. Jayakumar, Saji Mohandas, Sushant Kumar, Kuldeep Sharma, S. Karunasagar, and E. N. Rajagopal 2020: NCUM Global NWP System: Version 6 (NCUM-G:V6), NMRF/TR/06/2020.
9. Kumar Sumit, Gibies George, Buddhi Prakash J., M. T. Bushair, S. Indira Rani and John P. George 2021: NCUM Global DA System: Highlights of the 2021 upgrade, NMRF/TR/05/2021.
10. Mitra, A. K., A. K. Bohra, M. N. Rajeevan and T. N. Krishnamurti, 2009: Daily Indian precipitation analyses formed from a merged of rain-gauge with TRMM TMPA satellite derived rainfall estimates, *J. of Met. Soc. of Japan*, 87A, 265-279.
11. Mitra, A. K., I. M. Momin, E. N. Rajagopal, S. Basu, M. N. Rajeevan and T. N. Krishnamurti, 2013, Gridded Daily Indian Monsoon Rainfall for 14 Seasons: Merged TRMM and IMD Gauge Analyzed Values, *J. of Earth System Science*, 122(5), 1173-1182.
12. Sharma K., S. Karunasagar and Raghavendra Ashrit 2020: CRA Verification of GFS and NCUM Rainfall Forecasts for Depression cases during JJAS 2018. /NMRF/RR/05/2020
13. Sharma, K., Ashrit, R., Kumar, S. et al. Unified model rainfall forecasts over India during 2007–2018: Evaluating extreme rains over hilly regions. *J Earth Syst Sci* 130, 82 (2021). <https://doi.org/10.1007/s12040-021-01595-1>
14. Srivastava A K, Rajeevan M and Kshirsagar S R 2009: Development of a high resolution daily gridded temperature data set (1969–2005) for the Indian region; *Atmos. Sci. Lett.* 10 249–254, <https://doi.org/10.1002/asl.232>
15. Stephenson D.B., B. Casati, C.A.T. Ferro and C.A. Wilson, 2008: The extreme dependency score: a non-vanishing measure for forecasts of rare events. *Meteorol. Appl.*, 15, 41-50.
16. Walters, D., and co-authors: The Met Office Unified Model Global Atmosphere 6.0/6.1 and JULES Global Land 6.0/6.1 configurations, *Geosci. Model Dev.*, 10, 1487–1520, <https://doi.org/10.5194/gmd-10-1487-2017>, 2017.
17. Wilks D S 2011 (eds) *Statistical methods in the atmospheric 807 sciences*; 3rd edn, Elsevier, 676p